Fractional statistics and quantum scaling properties of the integrable Penson-Kolb-Hubbard chain

Carlindo Vitoriano[1] and M. D. Coutinho-Filho[2]
[1]*Unidade Acadêmica de Garanhuns, Universidade Federal Rural de Pernambuco, 55296-901 Garanhuns, PE, Brazil*
[2]*Laboratório de Física Teórica e Computacional, Departamento de Física, Universidade Federal de Pernambuco, 50670-901 Recife, PE, Brazil*

(Received 6 June 2010; revised manuscript received 29 August 2010; published 30 September 2010)

We investigate the ground-state and low-temperature properties of the integrable version of the Penson-Kolb-Hubbard chain. The model obeys fractional statistical properties, which give rise to fractional elementary excitations and manifest differently in the four regions of the phase diagram U/t versus n, where U is the Coulomb coupling, t is the correlated hopping amplitude, and n is the particle density. In fact, we can find local pair formation, fractionalization of the average occupation number per orbital k, or U- and n-dependent average electric charge per orbital k. We also study the scaling behavior near the U-driven quantum phase transitions and characterize their universality classes. Finally, it is shown that in the regime of parameters where local pair formation is energetically more favorable, the ground state exhibits power-law superconductivity; we also stress that above half filling the pair-hopping term stabilizes local Cooper pairs in the repulsive-U regime for $U<U_{c1}=-2t\cos(n\pi/2)$.

DOI: 10.1103/PhysRevB.82.125126 PACS number(s): 71.10.Fd, 05.30.Pr, 71.30.+h

I. INTRODUCTION

Twenty years ago, Haldane[1] formulated a generalized dimensional-independent version of fractional statistics based on state counting methods, i.e., a generalized *exclusion* statistics, suitable to describe interacting many-particle systems in condensed matter. The elements of the statistical matrix interaction, $g_{\alpha\beta}$, are defined by the linear relation

$$\Delta D_\alpha = -\sum_\beta g_{\alpha\beta}\Delta N_\beta, \tag{1}$$

which determines the variation in the available single-particle states to species α, i.e., ΔD_α, caused by a set of allowed changes $\{\Delta N_\beta\}$ on the number of occupied single-particle states of the species (fractional elementary excitations). Subsequently, Wu[2] (see also Refs. 3 and 4) developed the notion of an ideal exclusion gas, whose thermodynamic properties interpolate continuously between that of a noninteracting Bose gas ($g_{\alpha\beta}=0$) and that of a noninteracting Fermi gas ($g_{\alpha\beta}=\delta_{\alpha\beta}$). In addition, this formalism has the advantage of including Bethe-Ansatz solvable models as a special case, where the two-body phase shift is transmuted into the statistical interaction.[4–8] The importance of generalized exclusion statistics, however, lies to a considerable extent in the several attempts to account for a variety of condensed-matter phenomena using generalized exclusion statistics, such as: fractional quantum Hall effect,[1,2,9] low-temperature properties of Luttinger liquids,[10] Mott insulator,[11] transport through a one-dimensional wire within the Landauer-Büttiker approach,[12] trapped two-dimensional Bose gas with a repulsive delta-function interaction,[13] and adsorption of polyatomics.[14] Further, other Hamiltonian models obeying fractional exclusion statistics have been studied, such as: multicomponent Sutherland model,[15] quantum Calogero model,[16] model describing one-dimensional relativistic fermions interacting with the Toda array of N scalar fields,[17] Hubbard model with infinite-range interaction,[18] exclusion statistics and signature of strongly interacting anyons,[19] strongly interacting one-dimensional Bose gas,[20] gas of neutral fermionic atoms at ultralow temperatures with the attractive interaction tuned to Feshbach resonance,[21] phase transitions and pairing signature in strongly attractive Fermi atomic gases,[22] entanglement entropy in the Calogero-Sutherland model,[23] statistical correlations in an ideal gas of particles,[24] and many-spinon states and representations of Yangians in the SU(n) Haldane-Shastry model.[25]

Recently, the authors[26] have shown that the exactly solvable Hubbard chain with bond-charge interaction is mapped onto an ideal gas of three species of exclusons. Remarkably, the statistical matrix for this model with on-site interaction is the same found for the Hubbard model with infinite-range interaction.[18] In addition, we have shown that the map was crucial in clarifying several physical aspects of the model. On the other hand, considerable progress has been made to elucidate the underlying physics of the Hubbard model,[27] and several of its variants, after Anderson's suggestion[28] that the single-band Hubbard model could be the starting point to explain high-T_c superconductivity,[29] possibly associated with short-ranged pairing formation in real space. An interesting modified version of the Hubbard Hamiltonian that has been studied in order to turn light on this subject is the Penson-Kolb-Hubbard (PKH) model,[30–35] which is a variant of the model put forward by Penson and Kolb (PK),[36] just before the announcement of the discovery of high-T_c superconductivity, as an alternative to the attractive-U Hubbard model.

Since the proposal of the PK model, some controversy concerning the equivalence between the two above-referred models has been noticed in the context of numerical exact diagonalization and renormalization-group studies.[30,37] In any event, further strong evidence,[38,39] including also results using density-matrix renormalization-group and Luttinger-liquid approaches, point to the conclusion that the one-dimensional PK model at half filling with nonzero attractive

pair-hopping amplitude exhibits no phase transition (it takes place at zero pair-hopping amplitude Y, characterized by an essential singularity for the spin gap, $\Delta_s \propto e^{-\pi t/Y}$): the ground state (GS) displays nonzero (zero) spin (charge) gap with charge and superconducting correlation functions governed by power-law behavior, in agreement with results for the attractive-U Hubbard chain. On the other hand, in the repulsive case a spin-gap transition occurs at a finite value of the pair-hopping integral, such that the charge gap closes and a spin gap opens.[38]

These studies have been extended to higher dimensions and for electron densities away from half filling;[40,41] in the strong-coupling regime some discrepancies between the two models have been pointed out and attributed to the nonlocal pairing mechanism in the PK model. We also mention that rigorous results point to the equivalence of the models,[42] as far as the superconducting phase is concerned, and that in the PK model the superconducting condensation can only happen for η pairing at zero wave vector (local Cooper pairs).

The inclusion of Coulomb interactions, in addition to the pair-hopping term, as in PKH model,[30] opens the possibility of studying η-pairing induced superconductivity even in systems for which the standard Coulomb interactions are repulsive. In fact, the PKH model has been studied by several authors using a variety of techniques, such as, real-space renormalization group,[31] Bethe-Salpeter equation,[32] continuum-limit field theory (bosonization),[33] and Hartree-Fock approximation.[34,35]

We also stress that for the standard on-site repulsive Hubbard model Yang showed[43] that the η-pairing mechanism give rise to metastable states,[44] although the idea was largely used to obtain a more deep understanding of the Hubbard model[45,46] and to proposals of integrable extended repulsive or attractive Hubbard models with phases exhibiting stable η-pairing states.[47] Moreover, generalizations of η pairing for high-spin fermions have been suggested,[48] and the connection between η-pairing quantum entanglement and off-diagonal long-range order clarified.[49] Lastly, in an experimental context, it has been suggested[50] that η pairing, with nonzero momentum of the Cooper pairs, and d-wave superconductivity may coexist in the Fulde-Ferrel-Larkin-Ovchinnikov phase.

In this work, we consider the integrable version of the PKH chain.[51] In Sec. II this model Hamiltonian is introduced and its mapping onto an ideal excluson gas is discussed. In Sec. III the GS phase diagram of the model is analyzed and its quantum phases characterized with the help of fractional statistics concepts. In particular, we calculate the η-pairing correlation function at zero wave vector[43] and the GS energy as a function of the twisted angle in the boundary conditions. Section IV is devoted to obtain the universality class of the several quantum phase transitions exhibited by the model. Finally, concluding remarks follow in Sec. V.

II. MODEL AND EXCLUSION REPRESENTATION

The model we consider is defined on a linear chain of L sites and expressed by the Hamiltonian[51]

$$\mathcal{H} = -t \sum_{\langle i,j\rangle,\sigma} (1-n_{i\bar{\sigma}}) c_{i\sigma}^{\dagger} c_{j\sigma} (1-n_{j\bar{\sigma}}) + U \sum_i n_{i\uparrow} n_{i\downarrow} + Y \sum_{\langle i,j\rangle} c_{i\uparrow}^{\dagger} c_{i\downarrow}^{\dagger} c_{j\downarrow} c_{j\uparrow} - h \sum_i (n_{i\uparrow} - n_{i\downarrow}), \tag{2}$$

where $\langle i,j\rangle$ denotes nearest-neighbors sites, $c_{i\sigma}(c_{i\sigma}^{\dagger})$ are electron annihilation (creation) operators, $n_{i\sigma}=c_{i\sigma}^{\dagger}c_{i\sigma}$ is the number operator, $\sigma=\uparrow,\downarrow$, $\bar{\sigma}\equiv-\sigma$, t is the correlated hopping amplitude, which allows motion of electrons from singly occupied sites to empty ones only,[51] U is the on-site Coulomb interaction,[30] Y is the pair-hopping amplitude,[36] and $h=g\mu_B H/2$ (g is the gyromagnetic factor and μ_B is the Bohr magneton) is the interaction energy with the external magnetic field along the z direction (not considered in Ref. 51). We remark that the pair-hopping term stem from the off-diagonal contribution of the Coulomb interaction in a general tight-binding Hamiltonian as originally analyzed by Hubbard,[27,31] i.e., $Y=\langle ii|e^2/r|jj\rangle$. Attractive ($Y<0$) intersite pair hopping has been suggested to occur through various mechanisms, such as, electron-lattice coupling or hybridization effect.[52] From now on, we confine to the case

$$Y = -t \tag{3}$$

so that the resulting model is exactly solvable.[51] In this case, under open boundary condition, any sequence of $\uparrow$, $\downarrow$, and $\uparrow\downarrow$ spins is a preserved quantity and labels invariant subspaces of $\mathcal{H}$.[51] Let

$$N_1 = \sum_i n_{i\uparrow}(1-n_{i\downarrow}), \quad N_2 = \sum_i n_{i\downarrow}(1-n_{i\uparrow}),$$

$$N_3 = \sum_i n_{i\uparrow} n_{i\downarrow} \tag{4}$$

be the total number of single-up, single-down, and doubly occupied sites, respectively. The spectrum in each invariant subspace in the thermodynamic limit thus reads[51]

$$E(N_A,N) = \sum_k \varepsilon_k n_k + UN_3 - h(N_1 - N_2), \tag{5}$$

where $\{n_k\}$ are Fermi quantum numbers, $n_k=0,1$ per orbital, with $k=\frac{2\pi}{L}\nu(\nu=-\frac{L}{2}+1,\ldots,\frac{L}{2})$, and

$$\varepsilon_k = -2t\cos k. \tag{6}$$

Notice that the first term in Eq. (5) has a spinless character. The total number of particles is given by

$$N = N_1 + N_2 + 2N_3 \tag{7}$$

and

$$\sum_k n_k = N_1 + N_2 + N_3 \equiv N_A, \tag{8}$$

where N_A is the total number of singly and doubly occupied sites. At fixed N_1, N_2, and N_3 the degeneracy of E is determined by

$$g(N_1,N_2,N_3) = \frac{N_A!}{N_1!N_2!N_3!}. \tag{9}$$

Note that, since $N_2=N_A-N_1-N_3$,

$$\sum_{N_1=0}^{N_A-N_3} g(N_1,N_2,N_3) = 2^{2N_A-N}\binom{N_A}{N-N_A} \tag{10}$$

is the degeneracy of E in zero field and at fixed $N_3=N-N_A$ [see Eq. (8) of Ref. 51]. In the presence of a magnetic field, the grand-canonical partition function can be written in the form

$$\mathcal{Z}(\beta,\mu,h;U) = \sum_{N_A=0}^{+\infty}\sum_{N_3=0}^{N_A}\sum_{N_1=0}^{N_A-N_3}\frac{N_A!e^{-\beta(E-\mu N)}}{N_1!(N_A-N_3-N_1)!N_3!}, \tag{11}$$

where $\beta=1/(k_BT)$ is the inverse temperature, μ is the chemical potential, and $E-\mu N=\Sigma_k(\varepsilon_k-\mu+h)n_k+(U-h-\mu)N_3-2hN_1$. This sum is evaluated at once by using the binomial theorem

$$\mathcal{Z}(\beta,\mu,h;U) = \sum_{\{n_k\}} e^{-\beta\Sigma_k(\varepsilon_k-\mu_{eff})n_k} = \prod_k [1+e^{-\beta(\varepsilon_k-\mu_{eff})}], \tag{12}$$

where

$$\mu_{eff}(\beta,\mu,h;U) = \mu + \frac{1}{\beta}\ln[2\cosh(\beta h) + e^{-\beta(U-\mu)}]. \tag{13}$$

As expected, for $h=0$ this effective chemical potential reduces to that reported in Ref. 51.

In Ref. 26, the authors have pointed out that the thermodynamic properties of the model in Eq. (2) is that of an ideal excluson gas with three fractional species, $\langle n_{k,\alpha}\rangle$,

$$\langle N_\alpha\rangle \equiv \sum_k \langle n_{k,\alpha}\rangle, \tag{14}$$

identified as single-up ($\alpha=1$), single-down ($\alpha=2$), and paired ($\alpha=3$) carriers, coupled by the statistical matrix

$$[g]_{kk';\alpha\alpha'} = \delta_{kk'}\begin{pmatrix}1 & 1 & 1\\ 0 & 1 & 1\\ 0 & 0 & 1\end{pmatrix} \tag{15}$$

with corresponding species energies $\varepsilon_{k,\alpha}$, where

$$\varepsilon_{k,1} = \varepsilon_k - h - \mu, \tag{16}$$

$$\varepsilon_{k,2} = \varepsilon_k + h - \mu, \tag{17}$$

$$\varepsilon_{k,3} = \varepsilon_k + U - 2\mu. \tag{18}$$

We remark that the energy of species 3 has an additional dispersive contribution, ε_k, which precludes any condensation phenomenon, as observed in the Hubbard model with bond-charge interaction studied in Ref. 26. Clearly, the first term of the product form in Eq. (15), i.e., $\delta_{kk'}$, gives a fermionic character to the momentum degrees of freedom while the 3×3 matrix represents nontrivial effects associated with spin degrees of freedom. In fact, the grand canonical free energy is given by

$$\begin{aligned}\Omega &= -\frac{1}{\beta}\sum_{k,\alpha}\ln(1+w_{k,\alpha}^{-1})\\ &= -\frac{1}{\beta}\sum_{k}\ln(1+e^{-\beta\varepsilon_{k,1}}+e^{-\beta\varepsilon_{k,2}}+e^{-\beta\varepsilon_{k,3}})\\ &= -\frac{1}{\beta}\ln\mathcal{Z},\end{aligned} \tag{19}$$

where $\mathcal{Z}$ is given by Eq. (12) and $w_{k,\alpha}$ satisfies the Haldane-Wu distribution[1,2]

$$(1+w_{k,\alpha})\prod_{\lambda=1}^{3}\left(\frac{w_{k,\lambda}}{1+w_{k,\lambda}}\right)^{g_{\lambda\alpha}} = e^{\beta\varepsilon_{k,\alpha}}. \tag{20}$$

We can also verify that the thermal average occupation number of the fractional species, $\langle n_{k,\alpha}\rangle$, satisfies the exclusion relation[2]

$$\langle n_{k,\alpha}\rangle w_{k,\alpha} = 1 - \sum_{\lambda=1}^{3} g_{\alpha\lambda}\langle n_{k,\lambda}\rangle, \tag{21}$$

where

$$\langle n_{k,\alpha}\rangle = \frac{e^{-\beta\varepsilon_{k,\alpha}}}{1+\sum_{\lambda=1}^{3} e^{-\beta\varepsilon_{k,\lambda}}}, \tag{22}$$

$$\langle n_k\rangle = \frac{1}{e^{\beta(\varepsilon_k-\mu_{eff})}+1}, \tag{23}$$

and the grand-canonical energy reads

$$\langle E\rangle - \mu\langle N\rangle = \sum_{k,\alpha}\varepsilon_{k,\alpha}\langle n_{k,\alpha}\rangle. \tag{24}$$

We remark that $\langle n_k\rangle$ obeys a Fermi-type distribution with μ_{eff} given by Eq. (13).

III. GROUND-STATE PHASE DIAGRAM AND FRACTIONAL ELEMENTARY EXCITATIONS

In Fig. 1(a) we show the GS phase diagram in zero field calculated in the $U/t-n$ plane,[51] where $n\equiv N/L$ is the particle density, obtained by minimizing the GS energy with respect to the fractional species; note the absence of particle-hole symmetry around $n=1$. In this figure,

$$\frac{U_{c1}}{t} = -2\cos\left(\frac{n\pi}{2}\right), \quad \frac{U_{c2}}{t} = -2\cos(n\pi), \quad \frac{U_{c3}}{t} = 2 \tag{25}$$

are critical lines separating distinct quantum phases and U_{c2} and U_{c3} intersect at the quantum critical point (QCP). The plot of the chemical potential as a function of n is illustrated in Fig. 1(b) for $U=t$. Note that the plateau is associated with

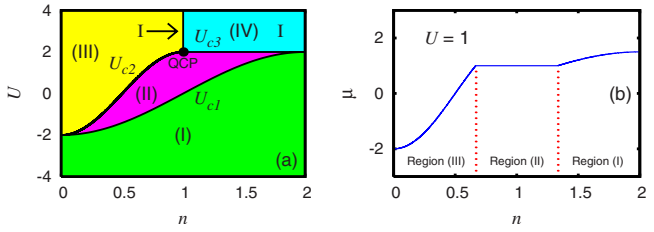

FIG. 1. (Color online) (a) GS phase diagram in zero field (see Ref. 51). Capital letters I denote insulating phases, otherwise the GS is metallic. Lines U_{c1} and U_{c2} are associated with MMT while line U_{c3} and the QCP are associated with MIT. (b) GS chemical potential as a function of the band filling. The region of plateau corresponds to values of n in region (II), being associated to large fluctuations in k space. (Energies in units of t.)

region (II), and its edges separate region (II) from regions (I) and (III) (see Ref. 51, including temperature effects).

Region (I) is a nonentropic metallic phase (however, see the η-pairing correlation function below) in which only the fractional species 3 is energetically favorable

$$\langle n_{k,1}\rangle = \langle n_{k,2}\rangle = 0, \tag{26}$$

$$\langle n_{k,3}\rangle = \theta(U_{c1} - \varepsilon_k), \tag{27}$$

where $\theta(x)$ is the step function. Therefore, the Fermi surface is defined by the k vectors $\{\pm k_{F1}\}$, where

$$k_{F1} = \frac{n\pi}{2}. \tag{28}$$

The GS energy per site is obtained from Eqs. (5) and (28)

$$\frac{E_1(n)}{L} = \int_{-k_{F1}}^{k_{F1}} \frac{dk}{2\pi}\varepsilon_k + \frac{nU}{2} = -\frac{2t}{\pi}\sin(n\pi/2) + \frac{nU}{2} \tag{29}$$

and the GS chemical potential is given by

$$\mu_1(n) = \frac{\partial(E_1/L)}{\partial n} = \frac{U}{2} - t\cos(n\pi/2). \tag{30}$$

As expected, Eqs. (29) and (30) are in agreement with Eq. (24). Thus, the GS charge compressibility

$$\kappa_1^{-1}(n) = \left(\frac{\partial\mu_1}{\partial n}\right)_{T=0} = \frac{\pi t}{2}\sin(n\pi/2) \tag{31}$$

is finite inside region (I) as well as in the limit $U \to U_{c1}^-$. A plot of the corresponding fractional elementary excitations (FEE) for this phase is shown in Fig. 2(a), for $n=2/3$ and $U=-5t$. In this figure, all k states in the interval $[-k_{F1}, k_{F1}]$ are occupied; this band of exclusons 3 is separated from the twofold spin-degenerate dispersive bands of exclusons 1 and 2 by the gap

$$\Delta_1 = \mu_1 - U \tag{32}$$

so that charge gapless excitations are composed of excitations of species 3 across the Fermi surface $\{\pm k_{F1}\}$. Notice that in region (I) the system is characterized by zero (nonzero) charge (spin) gap, in agreement with results for the PK model.[38]

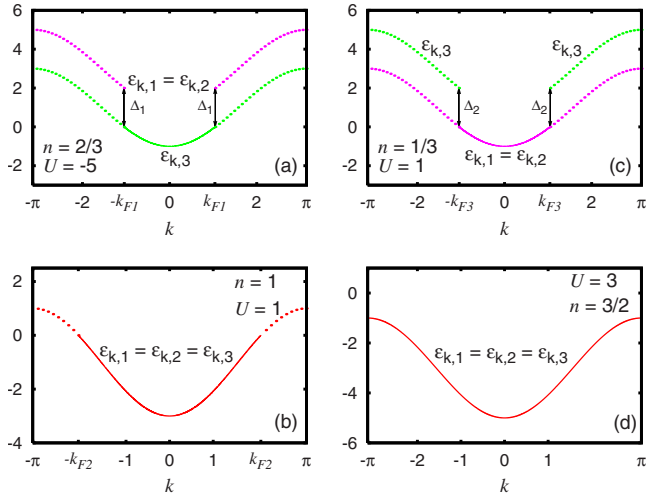

FIG. 2. (Color online) Fractional elementary excitations in zero field. (a) In region (I), a gap $\Delta_1=2$ separates the band of exclusion 3 from the empty degenerate band of exclusions 1 and 2. (b) In region (II), the degenerate band of exclusions 1, 2, and 3 give rise to an effective spinless band. (c) In region (III), a gap $\Delta_2=2$ separates the effective spinless band of exclusions 1 and 2 from the band of exclusions 3 empty. (d) In region (IV), the hopping motion is frozen and then the GS is insulating. (Energies in units of t.)

The η-pairing correlation function for *local* Cooper pairs

$$G_\eta(j,m) = \langle\Psi_0|c_{m\downarrow}^\dagger c_{m\uparrow}^\dagger c_{j\uparrow} c_{j\downarrow}|\Psi_0\rangle, \tag{33}$$

where $|\Psi_0\rangle$ is the GS of the system, allows us to test the GS superconducting properties in region (I). In order to calculate $G_\eta(j,m)$, it is useful to use a Jordan-Wigner-type transformation

$$d_j \equiv \exp\left[\frac{i\pi}{2}\sum_{l=1}^{j-1}(n_{l\uparrow} + n_{l\downarrow})\right] c_{j\uparrow} c_{j\downarrow}, \tag{34}$$

which, acting in the subspace with no single carrier, satisfies the anticommutation rules for fermionic operators: $\{d_j, d_m\} = \{d_j^\dagger, d_m^\dagger\} = 0$ and $\{d_j^\dagger, d_m\} = \delta_{j,m}$. At low temperatures, these local Cooper pairs obey a Fermi-type distribution, as in the attractive-U Hubbard chain,[53] with effective chemical potential [using Eq. (30) in Eq. (13)]

$$\mu_{eff,1} = -2t\cos k_{F1} + \mathcal{O}(k_B T)^2. \tag{35}$$

In fact, this is consistent with our mapping onto an ideal gas of three species of exclusons and the fact that, in region (I) and low T, $\Sigma_k\langle n_k\rangle \simeq N_3$ [see Eqs. (8) and (23)]. In terms of the Fourier transform of $d_j^\dagger$, defined by

$$d_k^\dagger = \frac{1}{\sqrt{L}}\sum_m e^{ikm} d_m^\dagger, \tag{36}$$

the GS in region (I) reads

$$|\Psi_0\rangle = \prod_{|k|<k_{F1}} d_k^\dagger|0\rangle = \left(\frac{1}{\sqrt{L}}\right)^{N_3} \times \sum_{\{n_i\}} \{\det(k_1,k_2,\ldots,k_{N_3};n_1,n_2,\ldots,n_{N_3}) \times |n_1\downarrow\uparrow,n_2\downarrow\uparrow,\ldots,n_{N_3}\downarrow\uparrow\rangle\}, \quad (37)$$

where $1 \le n_1 < n_2 < \cdots < n_{N_3} \le L$ and

$$\det(k_1,k_2,\ldots,k_{N_3};n_1,n_2,\ldots,n_{N_3}) = \sum_P (-1)^p P\{e^{ik_1n_1}e^{ik_2n_2}\ldots e^{ik_{N_3}n_{N_3}}\}, \quad (38)$$

where P is a permutation operator which generate all possible permutations of $\{n_1,n_2,\ldots,n_{N_3}\}$ and p is the number of interchanges in P, as expected in view of the mapping of $\mathcal{H}$ onto a free spinless Fermi gas Hamiltonian with each exclusion 3 (local Cooper pair) carrying a charge $2e$ per orbital k

$$\mathcal{H} - U\sum_i n_{i\uparrow}n_{i\downarrow} \leftrightarrow -t\sum_{\langle i,j\rangle} d_i^\dagger d_j \equiv \mathcal{H}_{eff}, \quad (39)$$

and $|n_1\downarrow\uparrow,n_2\downarrow\uparrow,\ldots,n_N\downarrow\uparrow\rangle \leftrightarrow |n_1,n_2,\ldots,n_N\rangle$. Now it is straightforward to express $G_\eta(j,m)$ in terms of d_j and $c_{j\sigma}$

$$G_\eta(j,m) = \langle\Psi_0|d_m^\dagger d_j|\Psi_0\rangle - \langle\Psi_0|c_{m\downarrow}^\dagger c_{m\uparrow}^\dagger c_{j\uparrow}c_{j\downarrow} \times \left\{\exp\left[\frac{i\pi}{2}\sum_{l=m}^{j-1}(n_{l\uparrow}+n_{l\downarrow})\right]-1\right\}|\Psi_0\rangle, \quad (40)$$

where $m<j$ is assumed. In the thermodynamic limit, however, only the first expectation value survives (see Appendix A)

$$\lim_{L\to\infty} G_\eta(j,m) = \frac{1}{L}\sum_k e^{ik(j-m)}\langle\Psi_0|d_k^\dagger d_k|\Psi_0\rangle = \frac{\sin k_{F1}|j-m|}{\pi|j-m|}, \quad (41)$$

which endows to the correlation function a critical power-law behavior. On the other hand, the charge-density correlation function reads

$$\lim_{L\to\infty} G_c(j,m) = \langle d_j^\dagger d_j d_m^\dagger d_m\rangle - \langle d_j^\dagger d_j\rangle\langle d_m^\dagger d_m\rangle = -\left[\frac{\sin k_{F1}(j-m)}{\pi(j-m)}\right]^2, \quad (42)$$

which, as expected, coincides with that of the spinless free Fermi gas, since each exclusion 3 occupies only a single orbital k, i.e., $k_{F1}=N_3\pi/L$. The above results in Eqs. (41) and (42) are in full agreement with Luttinger liquid properties of the spinless Fermi gas.[54]

We now consider $\mathcal{H}_{eff}$, Eq. (39), on a ring with a twisted Φ in the boundary conditions

$$\mathcal{H}_{eff} = -t\left[\sum_{j=1}^{L-1}(d_j^\dagger d_{j+1} + d_{j+1}^\dagger d_j) + e^{-2i\Phi}d_L^\dagger d_1 + e^{2i\Phi}d_1^\dagger d_L\right], \quad (43)$$

after the transformations $c_{L\sigma}^\dagger c_{1\sigma} \to e^{-i\Phi}c_{L\sigma}^\dagger c_{1\sigma}$ and $c_{1\sigma}^\dagger c_{L\sigma} \to e^{i\Phi}c_{1\sigma}^\dagger c_{L\sigma}$. Notice the phases $\pm 2\Phi$ in Eq. (43) due to the charge $2e$ of exclusion 3. For $-\pi/2 \le \Phi < \pi/2$ and an odd number of doubly occupied sites N_3, the momentum distribution is symmetrical with respect to the origin, and thus the GS energy reads[55]

$$E_1(\Phi) = -2t\frac{\sin(N_3\pi/L)}{\sin(\pi/L)}\cos(2\Phi/L). \quad (44)$$

On the other hand, for even N_3 we may put E_1 in the form

$$E_1(\Phi) = -2t\frac{\sin[(N_3-1)\pi/L]}{\sin(\pi/L)}\cos(2\Phi/L) + 2t\sin(2\Phi/L)\sin(N_3\pi/L), \quad (45)$$

for $-\pi/2 \le \Phi < 0$, and

$$E_1(\Phi) = -2t\frac{\sin[(N_3-1)\pi/L]}{\sin(\pi/L)}\cos(2\Phi/L) - 2t\sin(2\Phi/L)\sin(N_3\pi/L), \quad (46)$$

for $0 \le \Phi < \pi/2$. However, $E_1(\Phi+\pi)=E_1(\Phi)$ is satisfied, as expected in a superconducting ring.[56] In Fig. 3(a), $E_1(\Phi)/E_1(0)$ is plotted against Φ for $L=10$ and odd N_3. For the sake of comparison, in Fig. 3(b) we plot the same curve for the free spinless Fermi gas with charge e per orbital k. The energy shift[57] (odd N_3)

$$E_1(\Phi) - E_1(0) = \frac{4t}{\pi}\sin(N_3\pi/L)\frac{\Phi^2}{L} + \mathcal{O}(1/L^3) \equiv D\frac{\Phi^2}{L} + \mathcal{O}(1/L^3) \quad (47)$$

allows to identify the GS Drude weight D as that of a free spinless Fermi gas with effective charge $2e$ per orbital k

$$D = \frac{4t}{\pi}\sin(N_3\pi/L), \quad (48)$$

and also the persistent current[58]

$$I(\Phi) = -\frac{\partial E_1}{\partial\Phi} = -\frac{4v_{F1}}{\pi L}\Phi, \quad -\frac{\pi}{2} \le \Phi < \frac{\pi}{2}, \quad (49)$$

where $v_{F1}=\partial\mu_{eff,1}/\partial k_{F1}=2t\sin(N_3\pi/L)$. In contrast, for even N_3 the persistent current reads[58]

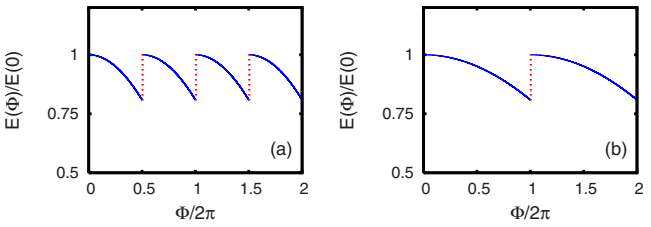

FIG. 3. (Color online) Normalized GS energy as a function of the twisted angle (a) for the integrable PKH model and (b) for the free spinless Fermi gas with charge e per orbital k. The number of sites is $L=10$.

$$I(\Phi) = -\frac{v_{F1}}{\pi L}\begin{cases} 4\Phi + 2\pi, & -\frac{\pi}{2} \le \Phi < 0, \\ 4\Phi - 2\pi, & 0 \le \Phi < \frac{\pi}{2}. \end{cases} \tag{50}$$

In closing our analysis of the GS superconducting properties in region (I), it is clear that the associated phenomena do not sustain in the thermodynamic limit.[59] However, in a mesoscopic scale our results are an interesting example of power-law superconductivity in a soluble model of strongly correlated electrons, whose elementary excitations obey fractional statistics. In a more realistic context, we should mention the recent successful efforts in measuring persistent currents in normal metal rings at very low T,[60] in agreement with earlier theoretical predictions.[61]

In region (II) the three fractional species coexist in equilibrium in a metallic phase. In fact, using the chemical potential[51] [see also Eqs. (B1), (B5), and (B6) in Appendix B]

$$\mu_2(T,n) = U + k_B T \ln\left[\frac{2(n-n^*)}{2n^*-n}\right] + \cdots, \tag{51}$$

where

$$n^* = \frac{1}{\pi}\arccos(-U/2t), \tag{52}$$

in Eq. (22), we find

$$\langle n_{k,1}\rangle_{T=0} = \langle n_{k,2}\rangle_{T=0} = \left(\frac{2n^*-n}{2n^*}\right)\theta(U-\varepsilon_k), \tag{53}$$

$$\langle n_{k,3}\rangle_{T=0} = \left(\frac{n-n^*}{n^*}\right)\theta(U-\varepsilon_k). \tag{54}$$

Therefore, the Fermi surface is defined by $\{\pm k_{F2}\}$, where

$$k_{F2} = n^*\pi. \tag{55}$$

The GS energy per site is

$$\frac{E_2(n)}{L} = \int_{-k_{F2}}^{k_{F2}} \frac{dk}{2\pi}\varepsilon_k + U\int_{-k_{F2}}^{k_{F2}} \frac{dk}{2\pi}\langle n_{k,3}\rangle_{T=0}$$

$$= -\frac{2t}{\pi}\sin(n^*\pi) + (n-n^*)U, \tag{56}$$

and thus the GS chemical potential is $\mu_2 = U$ [see Fig. 1(b)], in agreement with the $T \to 0$ limit of Eq. (51). Hence the GS charge compressibility $\kappa_2^{-1} = 0$ is singular.[51] However, this singularity is not related to a spatial phase separation due to absence of large fluctuations in density.[62] In fact, it has been noted[51] that κ_2 diverges as T^{-1}

$$\kappa_2(T,n) = \frac{(n-n^*)(2n^*-n)}{k_B T n^*} + \cdots, \tag{57}$$

where use of Eq. (51) has been made. After inserting Eq. (57) into the well-known result from the fluctuation-dissipation theorem[62]

$$(\Delta N)^2 \equiv \langle N^2\rangle - \langle N\rangle^2 = k_B T L \kappa_2, \tag{58}$$

we find that $\lim_{T\to 0} \Delta N \propto \sqrt{L}$ so the fluctuations of density lie within a peak centered around n. Notwithstanding, the singularity in κ_2 is caused by the GS entropy manifested in the distribution of occupation of exclusions in order to fill an orbital k [see Fig. 2(b) and entropy below] with average occupation numbers given by Eqs. (53) and (54). Indeed, each k state in the interval $[-k_{F2}, k_{F2}]$ is occupied either by exclusions 1 and 2 with equal probability given by

$$p_1 = p_2 = 1 - \frac{n}{2n^*} \tag{59}$$

or by exclusons 3 with probability

$$p_3 = \frac{n}{n^*} - 1, \tag{60}$$

in agreement with Eqs. (53) and (54), respectively, such that

$$\langle n_{k,1}\rangle_{T=0} + \langle n_{k,2}\rangle_{T=0} + \langle n_{k,3}\rangle_{T=0} = 1, \tag{61}$$

as required by Eqs. (8) and (23) for $\mu_{eff,2}(T=0) = U$. The GS entropy $S = -(\partial F/\partial T)_{T=0}$, where $F = \mu N + \Omega$ is the Helmholtz free energy [see Eq. (B8) in Appendix B] reads

$$S = k_B \ln\left[2^{\langle N_1\rangle + \langle N_2\rangle}\frac{\langle N_A\rangle!}{(\langle N_1\rangle + \langle N_2\rangle)!\langle N_3\rangle!}\right], \tag{62}$$

where use of the Stirling approximation $\ln N! = N\ln(N/e)$ and [see Eqs. (53) and (54)]

$$\langle N_1\rangle_{T=0} = \sum_k \langle n_{k,1}\rangle_{T=0} = \left(\frac{2n^*-n}{2}\right)L = \langle N_2\rangle_{T=0}, \tag{63}$$

$$\langle N_3\rangle_{T=0} = \sum_k \langle n_{k,3}\rangle_{T=0} = (n-n^*)L, \tag{64}$$

have been made. Note that $2^{\langle N_1\rangle + \langle N_2\rangle}$ counts the total spin degeneracy while the remaining term enclosed between square brackets is due entirely to degeneracy of the available states in k space. In this phase, the three dispersive bands of exclusons collapse into an effective single band of spinless fermions, as illustrated in Fig. 2(b) for $n=1$, $U=t$, and $k_{F2} = n^*\pi (= 2\pi/3)$; gapless excitations are composed by excitations of the three species of exclusons across the Fermi surface $\{\pm k_{F2}\}$. We also emphasize that formula (62) applies to all phases illustrated in Fig. 1(a) and confirms that in region (I) the entropy is zero.

A striking consequence of the GS entropy is better discussed in connection with the index characterizing the nature of the Fermi-surface singularity.[63] The Fermi surface suitable to electronic systems exhibiting non-Fermi-liquid behavior is defined by the k vectors that mark singularities in

$$\langle n_{k\uparrow}\rangle_{T=0} \equiv \langle n_{k,1}\rangle_{T=0} + \langle n_{k,3}\rangle_{T=0} \tag{65}$$

and

$$\langle n_{k\downarrow}\rangle_{T=0} \equiv \langle n_{k,2}\rangle_{T=0} + \langle n_{k,3}\rangle_{T=0}, \tag{66}$$

(in our case, step discontinuities at $k = \pm k_{F2}$). In zero field, we obtain with help of Eqs. (53) and (54)

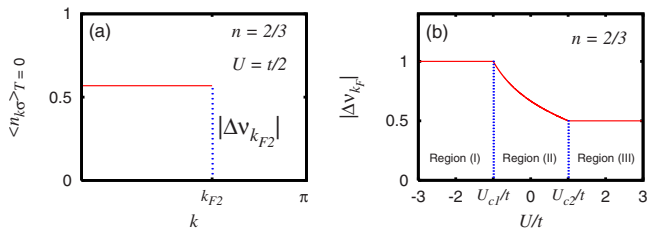

FIG. 4. (Color online) (a) Fractional average number of electrons of spin $\sigma=\uparrow,\downarrow$ in region (II) displaying step singularity of magnitude $|\Delta\nu_{k_{F2}}|$ at the wave vector k_{F2}. (b) Magnitude of the step singularity in $\langle n_{k\sigma}\rangle_{T=0}$ across regions (I), (II), and (III).

$$\langle n_{k\uparrow}\rangle_{T=0}=\langle n_{k\downarrow}\rangle_{T=0}=\frac{n}{2n^*}\theta(U-\varepsilon_k)\equiv|\Delta\nu_{k_{F2}}|\theta(U-\varepsilon_k), \tag{67}$$

where

$$\Delta\nu_{k_{F2}}=\lim_{\eta\to 0^+}[\langle n_{k_{F2}-\eta,\sigma}\rangle_{T=0}-\langle n_{k_{F2}+\eta,\sigma}\rangle_{T=0}] \tag{68}$$

characterizes the step singularities. In Fig. 4(a) we plot $\langle n_{k\sigma}\rangle_{T=0}$ as a function of k for $n=2/3$ and $U=t/2$ and in Fig. 4(b) we plot $|\Delta\nu_{k_F}|$ versus U/t for $n=2/3$ [extended to regions (I) and (III)]. Note that the average electric charge per orbital k is U dependent only for $U_{c1}<U<U_{c2}$

$$\begin{aligned}\langle Q\rangle &= e\langle n_{k,1}\rangle_{T=0}+e\langle n_{k,2}\rangle_{T=0}+2e\langle n_{k,3}\rangle_{T=0}\\ &= e\langle n_{k\uparrow}\rangle_{T=0}+e\langle n_{k\downarrow}\rangle_{T=0}\\ &= 2e|\Delta\nu_{k_{F2}}|,\end{aligned} \tag{69}$$

which interpolates between the integral values $2e$ [region (I)] and e [region (III)]. It is particularly interesting that we can express the average electric charge in terms of $|\Delta\nu_{k_{F2}}|$ only, since this result is well consistent with the original theoretical arguments of Haldane.[63]

In region (III) the fractional species 3 is absent, i.e., $\langle n_{k,3}\rangle_{T=0}=0$, and we should note the fractional occupation of the species 1 and 2

$$\langle n_{k,1}\rangle_{T=0}=\langle n_{k,2}\rangle_{T=0}=\frac{1}{2}\theta(U_{c2}-\varepsilon_k), \tag{70}$$

which implies the Fermi surface $\{\pm k_{F3}\}$, where

$$k_{F3}=n\pi. \tag{71}$$

The GS is equivalent to that of the $U=\infty$ Hubbard chain,[51] i.e., the phase is metallic with the GS entropy given by [see Eq. (62)]

$$S_3=k_B\ln 2^{\langle N_1\rangle+\langle N_2\rangle}, \tag{72}$$

the total energy per site reads

$$\frac{E_3(n)}{L}=-\frac{2t}{\pi}\sin(n\pi), \tag{73}$$

and

$$\mu_3(n)=-2t\cos(n\pi). \tag{74}$$

Note that the charge compressibility inside region (III) is finite: $\kappa_3^{-1}(n)=2\pi t\sin(n\pi)$ with $\lim_{U\to U_{c2}^+}\kappa_3^{-1}(n)=\lim_{n\to n^*}\kappa_3^{-1}(n)=\pi\sqrt{4t^2-U_{c2}^2}$ [see Eq. (52)]. In Fig. 2(c) a plot of the FEE for this metallic phase is depicted for $n=1/3$, $U=t$, and $k_{F3}=n\pi(=\pi/3)$. It should be noticed that the effective single band of spinless fermions is filled by exclusons 1 and 2 in the interval $[-k_{F3},k_{F3}]$; the gap

$$\Delta_2=U-\mu_3 \tag{75}$$

separates this band from that of empty exclusons 3.

Finally, in region (IV) the hopping motion is frozen and then the GS is equivalent to that of the Hubbard chain in the atomic limit.[51] The three fractional species coexist with GS average occupation numbers given by

$$\langle n_{k,1}\rangle_{T=0}=\langle n_{k,2}\rangle_{T=0}=\frac{2-n}{2}, \tag{76}$$

$$\langle n_{k,3}\rangle_{T=0}=n-1, \tag{77}$$

for $k\in(-\pi,\pi]$, which implies $\langle N_A\rangle=L$, $\langle N_1\rangle+\langle N_2\rangle=2L-N$, and $\langle N_3\rangle=N-L$. Therefore, the phase is insulating with GS entropy [Eq. (62)] given by

$$S_4=k_B\ln\left[2^{2L-N}\frac{L!}{(2L-N)!(N-L)!}\right], \tag{78}$$

the total energy per site is

$$\frac{E_4(n)}{L}=(n-1)U, \tag{79}$$

since the kinetic term in Eq. (5) vanishes, and $\mu_4=U$. In Fig. 2(d) a plot of the FEE for this full band insulating phase is shown for $n=3/2$ and $U=3t$.

Now, following the development presented for region (II), here with $n^*=1$, we find, using Eqs. (59) and (60)

$$p_1=p_2=1-\frac{n}{2} \tag{80}$$

and

$$p_3=n-1, \tag{81}$$

which implies the following average charge per orbital k:

$$\langle Q\rangle=ne, \tag{82}$$

as expected, this n-dependent result can also be obtained with help of Eqs. (76) and (77).

IV. SCALING PROPERTIES

We now provide a scaling study of the U-driven quantum phase transitions exhibited by Hamiltonian (2). The scaling form of F in the vicinity of a quantum critical point when $U-U_c$ is the dominant energy scale can be written as[59]

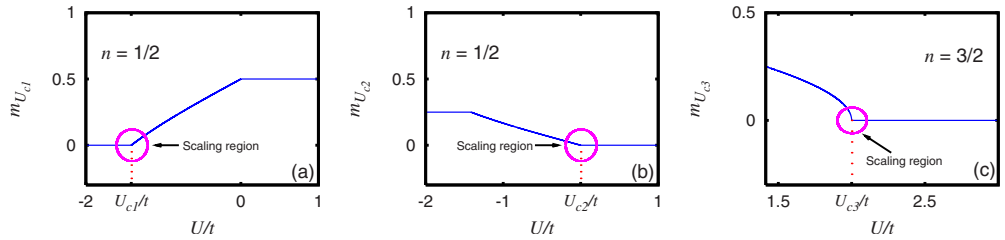

FIG. 5. (Color online) Typical plots of $m_{U_{c1}}$, $m_{U_{c2}}$, and $m_{U_{c3}}$ as a function of the normalized interaction. These quantities exhibit the proper behavior to signal [(a) and (b)] the U-driven MMT and (c) the U-driven MIT.

$$\frac{F_{sing}}{L} = |U - U_c|^{2-\alpha} F_U\left(\frac{T}{|U-U_c|^{\nu z}}, \frac{h}{|U-U_c|^{\beta+\gamma}}\right), \quad (83)$$

where α, β, γ, ν, and z are critical exponents, $\phi \equiv \nu z$ is the crossover exponent, and the scaling relations $\nu z = \beta + \gamma$ and $2 - \alpha = \nu(d+z)$ hold. However, if $k_B T$ dominates the energy scale, one can also write[59]

$$\frac{F_{sing}}{L} = T^{1+(d/z)} F_T\left(\frac{|U-U_c|}{T^{1/(\nu z)}}, \frac{h}{T}\right), \quad (84)$$

where F_U and F_T are scaling functions.

Our starting point to calculate F_{sing} in the various regimes of interest is the grand-canonical free energy, Eq. (19), in the convenient form below

$$\Omega = -\frac{L}{\beta}\int_{-2t}^{2t} d\varepsilon \sigma(\varepsilon) \ln[1 + 2e^{-\beta(\varepsilon-\mu)} + e^{-\beta(\varepsilon+U-2\mu)}], \quad (85)$$

where

$$\sigma(\varepsilon) \equiv \frac{1}{L}\sum_k \delta(\varepsilon - \varepsilon_k) = \frac{1}{\pi\sqrt{4t^2 - \varepsilon^2}} \quad (86)$$

is the lattice density of states, followed by the elimination of μ in favor of n through

$$n = -\frac{1}{L}\left(\frac{\partial \Omega}{\partial \mu}\right), \quad (87)$$

F_{sing} is then derived from $F = \mu N + \Omega$ by neglecting nonsingular terms.

A. U-driven metal-metal transition

1. Transition between regions (I) and (II)

We shall begin by discussing the U-driven metal-metal transition (MMT) between phases (I) and (II) separated by the critical line $U = U_{c1}$ [see Fig. 1(a)].

In region (I), one has $e^{\beta(\mu-U)} \gg 1$ so that the simplified form $\Omega_1 \simeq -\frac{1}{\beta}\Sigma_k \ln[1 + e^{-\beta(\varepsilon_k + U - 2\mu)}]$ is sufficient to calculate the asymptotic form for F_1 *à la* Sommerfeld when $|U - U_{c1}|$ dominates the energy scale as $T \to 0$, i.e., $\mu_1 = \frac{U}{2} - t\cos(n\pi/2) + \frac{\pi^2 (k_B T)^2 \cos(n\pi/2)}{24 t \sin^2(n\pi/2)} + \cdots$. Therefore, the singular part of F inside region (I) and in the vicinity of the critical line $U = U_{c1}$ can be cast in the form

$$\frac{F_{sing,1}}{L} = -\frac{\pi (U - U_{c1})^2}{12 t \sin(n\pi/2)}\left[\left(\frac{k_B T}{U - U_{c1}}\right)^2 + \cdots\right], \quad (88)$$

which implies $\alpha = \gamma = 0$, $\beta = \nu = z = 1$, and crossover exponent $\phi = 1$. We note that $F_{sing,1}$ is dominated by gapless excitations around $k = k_{F1} = \frac{n\pi}{2}$ [see Fig. 2(a) as $\Delta_1 \to 0^+$]

$$\varepsilon_{k,\alpha=1,2,3} = (\varepsilon_k - U)_{U=U_{c1}} \simeq (2t \sin k_{F1})(k - k_{F1}) \sim (k - k_{F1})^z, \quad (89)$$

being consistent with the dynamical exponent $z = 1$. The specific heat $C = -\frac{T}{L}\left(\frac{\partial^2 F}{\partial T^2}\right)$ in region (I) follows from Eq. (88):

$$C_1 = \frac{\pi k_B^2 T}{6t \sin(n\pi/2)} + \cdots, \quad (90)$$

which is the low T free Fermi gas result, except for a (1/2) factor; indeed, although a excluson 3 carries two particles per orbital k (local Cooper pair), which explains the filling factor $(n/2)$, its kinetic energy is that of a spinless particle. Moreover, the thermal mass $m_T \propto C/T \sim |U - U_{c1}|^{2-\alpha-2\nu z}$ $(= |U - U_{c1}|^0)$ is consistent with the scaling prediction. On the other hand, we find that the spin susceptibility reads

$$\chi = -\frac{1}{L}\left(\frac{\partial^2 F}{\partial h^2}\right)_{h=0} = \lim_{h\to 0}\beta\frac{(\langle N_1\rangle + \langle N_2\rangle)_{T,h}}{L}, \quad (91)$$

which implies that this magnetic response is a measure of the average *local* magnetic moment defined by[51,64] $\lambda_0 = \lim_{L\to\infty}\langle \frac{1}{L}\Sigma_i (n_{i\uparrow} - n_{i\downarrow})^2\rangle = n - 2\langle N_3\rangle/L = (\langle N_1\rangle + \langle N_2\rangle)/L$. Therefore, in the same regime of Eq. (88), χ is exponentially small in region (I)

$$\chi_1 = \frac{n}{k_B T} e^{-|U_{c1} - U|/(2k_B T)} + \cdots, \quad (92)$$

due to the cost in energy (spin gap) $\Delta_1 = \mu_1 - U = |U - U_{c1}|/2$ separating the band of exclusons 3 from the twofold spin-degenerate dispersive bands of exclusons 1 and 2 [see Fig. 2(a)].

We now take

$$m_{U_{c1}} \equiv \frac{(\langle N_1\rangle + \langle N_2\rangle)_{T=0,h=0}}{L} \quad (93)$$

as the order parameter for this MMT, i.e., the GS expectation value of local magnetic moment. A plot of this quantity as a function of the normalized interaction is shown in Fig. 5(a) for $n = 1/2$. The critical behavior of $m_{U_{c1}}$ is obtained by noting that n^*, Eq. (52), can be expanded in powers of U/t in

the vicinity of the critical line $U=U_{c1}$, but now inside region (II)

$$n^* = \frac{n}{2} + \frac{U-U_{c1}}{2\pi t \sin(n\pi/2)} + \cdots . \tag{94}$$

Then, using Eq. (63), we obtain

$$m_{U_{c1}} = \frac{U-U_{c1}}{\pi t \sin(n\pi/2)} + \cdots , \quad U \to U_{c1}^{+}, \tag{95}$$

in agreement with $\beta=1$. Note, from the plot in Fig. 5(a), that $m_{U_{c1}}=0$ inside region (I), where $U<U_{c1}$.

On the other hand, in order to derive the singular part of F inside region (II) and in the vicinity of $U=U_{c1}$, we insert the expansion Eq. (94) into Eq. (B8) (see Appendix B) to obtain

$$\frac{F_{sing,2}}{L} = -\frac{(U-U_{c1})^2}{\pi t \sin(n\pi/2)} \left\{ \left(\frac{k_B T}{U-U_{c1}} \right)^2 \times \left[\frac{\pi^2}{12} + \ln^2\left(\frac{U-U_{c1}}{t} \right) \right] - \left(\frac{k_B T}{U-U_{c1}} \right) \ln\left(\frac{U-U_{c1}}{t} \right) + \cdots \right\}, \tag{96}$$

which implies the same universality class of $F_{sing,1}$ in Eq. (88); and that, unlike Eq. (90), in region (II) the specific heat and m_T display U-dependent scaling logarithmic correction, consistent with $d=z(=1)$ (Ref. 59) and with the special character of this singular ($\kappa^{-1}=0$) and entropic [see Eqs. (62)–(64)] metallic phase

$$C_2 = \frac{\pi k_B^2 T}{6t \sin(n\pi/2)} \left[1 + \frac{12}{\pi^2} \ln^2\left(\frac{U-U_{c1}}{t} \right) + \cdots \right]. \tag{97}$$

Moreover, the spin susceptibility reads

$$\chi_2 = \frac{U-U_{c1}}{\pi t k_B T \sin(n\pi/2)} - \frac{2}{\pi t \sin(n\pi/2)} \ln\left(\frac{U-U_{c1}}{t} \right) + \cdots , \tag{98}$$

which is derived after using Eqs. (94) and (B1)–(B7) in order to calculate $(\langle N_1\rangle + \langle N_2\rangle)_{T,h=0}$ [see Eq. (91)]. We stress that, although χ_2 in Eq. (91) is dominated by the U-induced Curie-type contribution, the Pauli component is the one to be identified with the expected scaling behavior $\chi_2 \sim |U-U_{c1}|^{-\gamma} (= |U-U_{c1}|^0)$, here enhanced by a U-dependent logarithmic factor.

We shall now consider the singular part of F at $U=U_{c1}$ and $T \to 0$ [see Eq. (C7) in Appendix C]

$$\frac{F_{sing,U_{c1}}}{L} = -\frac{(k_B T)^2}{4\pi t \sin(n\pi/2)} \left[\frac{\pi^2}{3} + \ln^2(r^2) \right] - \frac{n k_B T}{r} + \cdots , \tag{99}$$

where

$$r = \frac{A}{\lim_{l\to\infty} \alpha_l}, \quad A = \frac{\pi t n \sin(n\pi/2)}{2k_B T}, \tag{100}$$

and $\alpha_1 = \ln(A)$, $\alpha_{l+1} = \ln(A/\alpha_l)$ $(l=1,2,3,\ldots)$. As predicted by Eq. (84), one finds that $F_{sing}/L \sim T^{1+d/z} (=T^2)$ with T-dependent logarithmic singularities consistent with the $d=z(=1)$ case.[59] We can thus obtain the quantum critical behavior of the specific heat, $C \sim T^{d/z} (=T)$,

$$C_{U_{c1}} = \frac{\pi k_B^2 T}{6t \sin(n\pi/2)} \left[1 + \frac{12}{\pi^2} \ln^2\left(\frac{k_B T}{t} \right) + \cdots \right] \tag{101}$$

and of the spin susceptibility, using Eqs. (C1) and (C5) and proceeding as before, $\chi \sim T^{(d/z)-1} (=T^0)$

$$\chi_{U_{c1}} = \frac{2}{\pi t \sin(n\pi/2)} \ln\left(\frac{t}{k_B T} \right) + \cdots , \tag{102}$$

both at the line $U=U_{c1}$. We should notice that the above results for the specific heat and the susceptibility are Fermi-liquid like, but again the special character of the metallic phase in region (II) gives rise to T-dependent logarithmic singularities.

The vanishing behavior of $m_{U_{c1}}$ at $U=U_{c1}$ in the presence of a magnetic field, $h/t \ll 1$, defines the exponent δ

$$m_{U_{c1}}(h) = \frac{(\langle N_1\rangle + \langle N_2\rangle)_{T=0,h}}{L} = \lim_{T\to 0} \frac{1}{L} \sum_k (\langle n_{k,1}\rangle + \langle n_{k,2}\rangle)_{T,h} = \lim_{\beta\to\infty} \frac{1}{L} \sum_k \frac{1+e^{-2\beta h}}{e^{\beta(\varepsilon_k - h - \mu)} + 1 + e^{-2\beta h} + e^{\beta(\mu - h - U_{c1})}}, \tag{103}$$

where use of Eqs. (16)–(18) and (22) has been made. Next, we substitute $\mu = U_{c1} + h + \delta\mu$ in the above equation, with $X = \lim_{\beta\to\infty} e^{\beta\delta\mu}$ finite, to obtain

$$\frac{(\langle N_1\rangle + \langle N_2\rangle)_{T=0,h}}{L} = \frac{1}{X+1} \int_{-2t}^{U_{c1}+2h} d\varepsilon \sigma(\varepsilon) = \frac{1}{X+1} \left(\frac{n}{2} + \frac{h}{\pi t \sin(n\pi/2)} + \cdots \right). \tag{104}$$

The value of X is calculated by using Eq. (7)

$$n = \frac{(\langle N_1\rangle + \langle N_2\rangle)_{T=0,h}}{L} + 2\frac{\langle N_3\rangle_{T=0,h}}{L}, \tag{105}$$

where

$$\frac{\langle N_3\rangle_{T=0,h}}{L} = \frac{X}{X+1} \int_{-2t}^{U_{c1}+2h} d\varepsilon \sigma(\varepsilon) = \frac{X}{X+1} \left(\frac{n}{2} + \frac{h}{\pi t \sin(n\pi/2)} + \cdots \right) \tag{106}$$

and use of Eqs. (16)–(18) and (22) has also been made. Now, by inserting Eqs. (104) and (106) into Eq. (105), one obtains

after some algebra: $X=\pi tn\ \sin(n\pi/2)/4h$. Therefore,

$$m_{U_{c1}}(h)=\frac{2h}{\pi t\ \sin(n\pi/2)}+\cdots, \tag{107}$$

in agreement with the scaling prediction $\delta=1$.

2. Transition between regions (II) and (III)

We now consider the transition between metallic phases separated by the critical line $U=U_{c2}$. Inside region (III) one has $e^{\beta(\mu-U)}\ll 1$ and thus $\Omega_3\simeq-\frac{1}{\beta}\Sigma_k\ln[1+2e^{-\beta(\varepsilon_k-\mu)}]$ is the starting point to calculate the Sommerfeld-type expansion for F_3. The singular part of F inside region (III) when $|U-U_{c2}|$ dominates the energy scale reads

$$\frac{F_{sing,3}}{L}=-\frac{\pi(U-U_{c2})^2}{12t\ \sin(n\pi)}\left[\left(\frac{k_BT}{U-U_{c2}}\right)^2+\cdots\right], \tag{108}$$

which reduces to that of Eq. (88) by replacing $U_{c2}\to U_{c1}$ and $n\pi\to n\pi/2$. The reason for the later substitution is because the effective single band of spinless fermions in region (I) is formed by one exclusion 3 per orbital k while in region (III) each orbital k is filled by two exclusons, 1 and 2, both with fractional occupation 1/2. As a consequence, this U-driven MMT is in the same universality class of the above transition. If we approach the critical line $U=U_{c2}$ from region (III), C is now obtained from Eq. (108)

$$C_3=\frac{\pi k_B^2T}{6t\ \sin(n\pi)}+\cdots, \tag{109}$$

in agreement with the thermal response of a spinless Fermi gas. In the same regime, χ is dominated by the Curie response

$$\chi_3=\frac{n}{k_BT}+\cdots, \tag{110}$$

due to the cost in energy $\Delta_2=U-\mu_3=|U-U_{c2}|$ separating the effective single band of spinless fermions filled by exclusons 1 and 2 from the empty band of exclusons 3 [see Fig. 2(c) and Eq. (92) for the opposite case].

In contrast to the previous U-driven MMT, however, we take as the order parameter the quantity

$$m_{U_{c2}}=\frac{\langle N_3\rangle_{T=0}}{L}, \tag{111}$$

i.e., the GS density of doubly occupied sites, whose plot as a function of U/t for $n=1/2$ is shown in Fig. 5(b).

Inside region (II) and near the critical line $U=U_{c2}$, the singular part of F can be calculated by using the expansion

$$n^*=n-\frac{U_{c2}-U}{2\pi t\ \sin(n\pi)}+\cdots \tag{112}$$

into Eq. (B8) [note that similar calculation was made to obtain Eq. (96)]

$$\frac{F_{sing,2}}{L}=-\frac{(U_{c2}-U)^2}{4\pi t\ \sin(n\pi)}\left\{\left(\frac{k_BT}{U_{c2}-U}\right)^2\times\left[\frac{\pi^2}{3}+\ln^2\left(\frac{U_{c2}-U}{t}\right)\right]-2\left(\frac{k_BT}{U_{c2}-U}\right)\ln\left(\frac{U_{c2}-U}{t}\right)+\cdots\right\} \tag{113}$$

with corresponding U-dependent scaling logarithmic correction to the specific heat and thermal mass

$$C_2=\frac{\pi k_B^2T}{6t\ \sin(n\pi)}\left[1+\frac{3}{\pi^2}\ln^2\left(\frac{U_{c2}-U}{t}\right)+\cdots\right]. \tag{114}$$

In the same regime, the calculation of χ at low T is as follows. First, we calculate $(\langle N_1\rangle+\langle N_2\rangle)_{T,h=0}$ by using the Taylor expansion for μ, Eqs. (B1)–(B5), along with Eq. (112). So, by inserting the result in Eq. (91), we find

$$\chi_2=\frac{n}{k_BT}\left(1-\frac{U_{c2}-U}{\pi tn\ \sin(n\pi)}+\cdots\right)+\frac{1}{\pi t\ \sin(n\pi)}\ln\left(\frac{U_{c2}-U}{t}\right)+\cdots, \tag{115}$$

where both Curie and Pauli-type contributions with U-dependent corrections are found.

It is interesting to obtain F_{sing}/L at $U=U_{c2}$ [see Eq. (D8) in Appendix D]

$$\frac{F_{sing,U_{c2}}}{L}=-\frac{nk_BTx_1}{2}-\frac{(k_BT)^2}{4\pi t\ \sin(n\pi)}\left[\frac{\pi^2}{3}+\ln^2(2x_1)\right]+\cdots, \tag{116}$$

where $x_1=\lim_{k\to\infty}x_1^{(k)}$, $x_1^{(k+1)}=-\frac{k_BT\ln(2x_1^{(k)})}{n\pi t\ \sin(n\pi)}$, $k=0,1,2,3,\ldots$, and $x_1^{(0)}=\frac{2k_BT}{n\pi t\ \sin(n\pi)}$ are chosen to guarantee convergence. It follows that the quantum critical behavior of the specific heat is

$$C_{U_{c2}}=\frac{\pi k_B^2T}{6t\ \sin(n\pi)}\left[1+\frac{3}{\pi^2}\ln^2\left(\frac{k_BT}{t}\right)+\cdots\right], \tag{117}$$

which should be compared with the expression given by Eq. (101). The quantum critical behavior of the magnetic spin susceptibility, Eq. (91), is found by calculating $(\langle N_1\rangle+\langle N_2\rangle)_{T,h=0}$ using the chemical potential at $U=U_{c2}$ from Appendix D, and proceeding as in previous case

$$\chi_{U_{c2}}=\frac{n}{k_BT}+\frac{1}{\pi t\ \sin(n\pi)}\ln\left(\frac{k_BT}{t}\right)+\cdots. \tag{118}$$

Note that the Curie term dominates the magnetic response of the system; however, it is interesting to note that the negative Pauli term has the appropriate scaling dependence ($\chi\sim T^0$), enhanced by a T-dependent logarithmic singularity.

In the preceding discussion, we have performed the explicit calculation of the exponent δ based on the fact that $m_{U_{c1}}$ couples itself directly with the external magnetic field h [see Eq. (107)]. In the present case, however, there is an important difference since $m_{U_{c2}}=0$ at $U=U_{c2}$ and $T=0$. In

such case, the standard procedure is to add to the Hamiltonian $\mathcal{H}$ the term $-h_{U_{c2}}\Sigma_i n_{i\uparrow}n_{i\downarrow}$, where $h_{U_{c2}}$ is the scaling field coupled to $m_{U_{c2}}$. In fact, one does get

$$m_{U_{c2}} = \frac{h_{U_{c2}}}{2\pi t \sin(n\pi)} + \cdots, \tag{119}$$

in agreement with $\delta=1$.

B. *U*-driven metal-insulator transition

The critical line $U=U_{c3}$ separates the metallic phase [region (II)] from the insulating one [region (IV)]. Inside region (II) and near the critical line $U=U_{c3}$, the singular part of F at $n=1$ when $|U-U_{c3}|$ dominates the energy scale is obtained by using the expansion

$$n^* = 1 - \frac{1}{\pi}\left(\frac{U_{c3}-U}{t}\right)^{1/2} - \frac{1}{24\pi}\left(\frac{U_{c3}-U}{t}\right)^{3/2} + \cdots, \tag{120}$$

in Eq. (B8)

$$\frac{F_{sing,2}}{L} = -\left(\frac{2t}{3\pi}\right)\left(\frac{U_{c3}-U}{t}\right)^{3/2} \times\left\{1 - \frac{3}{4}\left(\frac{k_BT}{U_{c3}-U}\right)\ln\left(\frac{U_{c3}-U}{t}\right) + \frac{3}{8}\left(\frac{k_BT}{U_{c3}-U}\right)^2 \times\left[\frac{\pi^2}{3} + \frac{1}{4}\ln^2\left(\frac{U_{c3}-U}{t}\right)\right] + \cdots\right\}, \tag{121}$$

which implies that this metal-insulator transition (MIT) is in the same universality class as that of the spinless free Fermi gas:[18,26] $\alpha=\beta=\gamma=\nu=1/2$, $z=2$, and crossover exponent $\phi=1$. Note the U-dependent logarithmic corrections, even though in this case one has $d\neq z$. The exponent $z=2$ is consistent with gapless excitations around $k=k_{F2}=\pi$ [see Fig. 2(b)]

$$\varepsilon_{k,\alpha=1,2,3} = (\varepsilon_k - U)_{U=U_{c3}} \simeq -t(k-k_{F2})^2 \sim (k-k_{F2})^z. \tag{122}$$

The corresponding specific heat is

$$C_2 = \frac{k_B^2 T}{2\pi t}\left(\frac{U_{c3}-U}{t}\right)^{-1/2} \times\left[\frac{\pi^2}{3} + \frac{1}{4}\ln^2\left(\frac{U_{c3}-U}{t}\right)\right] + \cdots, \tag{123}$$

and the thermal mass $m_T \sim (U_{c3}-U)^{-1/2}\ln^2(\frac{U_{c3}-U}{t})$ is in agreement with scaling prediction $m_T \sim |U-U_{c3}|^{2-\alpha-2\nu z} (=|U-U_{c3}|^{-1/2})$.

Further, inside region (II), but away from half-filled band, i.e., $n-1 \gg (U_{c3}-U)/t$, the universality class of the U-driven MIT is the same as that for the $n=1$ case. In fact, using expansion Eq. (120) again in Eq. (B8), the singular part of F in the scaling region reads

$$\frac{F_{sing,2}}{L} = -\left(\frac{2t}{3\pi}\right)\left(\frac{U_{c3}-U}{t}\right)^{3/2} \times\left\{1 - \frac{3}{2}\left(\frac{k_BT}{U_{c3}-U}\right)\ln\left(\frac{4(n-1)}{(2-n)^2}\right) + \frac{3}{8}\left(\frac{k_BT}{U_{c3}-U}\right)^2 \times\left[\frac{\pi^2}{3} + \ln^2\left(\frac{4(n-1)}{(2-n)^2}\right)\right] + \cdots\right\}, \tag{124}$$

and the corresponding specific heat is given by

$$C_2 = \frac{k_B^2 T}{2\pi t}\left(\frac{U_{c3}-U}{t}\right)^{-1/2}\left[\frac{\pi^2}{3} + \ln^2\left(\frac{4(n-1)}{(2-n)^2}\right)\right] + \cdots, \tag{125}$$

where n-dependent logarithmic corrections should be noticed. The spin susceptibility in the scaling region is calculated by using expansion Eq. (120) in order to calculate μ; proceeding as before, we obtain

$$\chi_2 = \left(\frac{2-n}{k_BT}\right)\left[1 - \frac{2}{\pi(2-n)}\left(\frac{U_{c3}-U}{t}\right)^{1/2} + \cdots\right] + \frac{1}{\pi t}\left(\frac{U_{c3}-U}{t}\right)^{-1/2}\ln\left(\frac{4(n-1)}{(2-n)^2}\right) + \cdots, \tag{126}$$

whose scaling part is in agreement with $\gamma=1/2$.

For this transition, we take, in both cases ($n=1$ or $n>1$),

$$m_{U_{c3}} = \frac{\langle N_3\rangle_{T=0}}{L} - (n-1) \tag{127}$$

as the associated order parameter. The reason to subtract $n-1$ is that $\frac{\langle N_3\rangle_{T=0}}{L} = n-1$ at $U=U_{c3}$ [see Eq. (64) for $n^*=1$]. In Fig. 5(c), $m_{U_{c3}}$ versus normalized interaction is plotted for $n=3/2$. Note from the plot that $m_{U_{c3}}=0$ for $U\geq U_{c3}$. The critical behavior of the order parameter can be obtained at once by using Eq. (120) into Eq. (64)

$$m_{U_{c3}} = \frac{1}{\pi}\left(\frac{U_{c3}-U}{t}\right)^{1/2} + \cdots, \quad U\to U_{c3}^-, \tag{128}$$

in agreement with $\beta=1/2$.

We are now interested in obtaining the singular part of F at $U=U_{c3}$. Away from half-filled band ($n>1$), we find [see Eq. (E10) in Appendix E]

$$\frac{F_{sing,U_{c3}}}{L} = -\frac{t}{2\pi}\left(\frac{k_BT}{t}\right)^{3/2}\int_0^{+\infty}\frac{d\theta}{\sqrt{\theta}}\ln(1+e^{-\theta/y_0}) + \cdots, \tag{129}$$

where

$$y_0 = \frac{4(n-1)}{(2-n)^2}, \tag{130}$$

in accordance with Eq. (84) for $z=2$, i.e., $F_{sing,U_{c3}}/L \sim T^{3/2}$. We have also checked the prediction $F_{sing,U_{c3}}/L \sim T^{3/2}$ at $n=1$ (see Appendix E). It is interesting to write the explicit form of the corresponding quantum critical behavior of $C \sim T^{d/z} (=T^{1/2})$

$$C_{U_{c3}} = \frac{3k_B}{8\pi}\left(\frac{k_BT}{t}\right)^{1/2}\int_0^{+\infty}\frac{d\theta}{\sqrt{\theta}}\ln(1+e^{-\theta}/y_0) + \cdots \quad (131)$$

and of the scaling part of $\chi[\sim T^{d/z-1}(=T^{-1/2})]$

$$\chi_{U_{c3}} = \frac{2-n}{k_BT} - \frac{P}{t}\left(\frac{k_BT}{t}\right)^{-1/2} + \cdots, \quad (132)$$

where

$$P = \frac{2-n}{\pi}\left[\frac{(2-n)^2\sqrt{\pi}}{8(n-1)} + \frac{4n(n-1)}{(2-n)^3}\int_0^{\infty}\frac{e^{-\theta}\sqrt{\theta}}{(e^{-\theta}+y_0)^2}d\theta\right], \quad (133)$$

calculated by using Eqs. (E1) and (E5) in order to obtain the total number of single-up and single-down occupied sites in zero field, as required by Eq. (91).

Finally, it should be noticed that inside the Mott phase, in which $U>2t$, $n=1$, and $e^{\beta(\mu-U)}\ll 1$ (activated regime), F is given by

$$\frac{F_{Mott}}{L} = -k_BT\ln 2 - \frac{t}{\sqrt[4]{4\pi}}\left(\frac{k_BT}{t}\right)^{5/4}e^{-(U-2t)/2k_BT} + \cdots. \quad (134)$$

The corresponding specific heat thus reads [note the misprint in the signal of the (7/4) T power in Ref. 51]

$$C_{Mott} = \frac{k_B}{\sqrt[4]{4\pi}}\left(\frac{U-2t}{2t}\right)^2\left(\frac{k_BT}{t}\right)^{-7/4}e^{-(U-2t)/2k_BT} + \cdots. \quad (135)$$

We also remark that several additional features of the T-dependent specific heat were studied in great detail in Ref. 51.

Finally, as in Ref. 26, the scaling analysis of the model allows us to predict power law or logarithmic singularities associated with the critical lines using the scaling form for the free energy in Eq. (83): $\frac{1}{L}(\frac{\partial S}{\partial U})_{N,T=0}\sim|U-U_c|^{1-\alpha-\nu z}$. In fact, for the MMT $(1-\alpha-\nu z=0)$

$$\frac{1}{L}\left(\frac{\partial S}{\partial U}\right)_{N,T=0} = -\frac{k_B}{\pi t\sin(n\pi/2)}\ln\left(\frac{U-U_{c1}}{t}\right) + \cdots, \quad U\to U_{c1}^{+}, \quad (136)$$

$$\frac{1}{L}\left(\frac{\partial S}{\partial U}\right)_{N,T=0} = \frac{k_B}{2\pi t\sin(n\pi)}\ln\left(\frac{U_{c2}-U}{t}\right) + \cdots, \quad U\to U_{c2}^{-}, \quad (137)$$

and for the MIT $(1-\alpha-\nu z=-1/2)$

$$\frac{1}{L}\left(\frac{\partial S}{\partial U}\right)_{N,T=0} = \frac{k_B}{2\pi t}\left(\frac{U_{c3}-U}{t}\right)^{-1/2}\ln\left(\frac{4(n-1)}{(2-n)^2}\right) + \cdots, \quad U\to U_{c3}^{-}, \quad n>1. \quad (138)$$

Interestingly, universal properties of quantum phase transitions were studied in the framework of quantum-information theory,[65] where singularities similar to the ones above play a relevant role.

V. SUMMARY AND DISCUSSION

In this paper we have studied the GS and low-temperature properties of the integrable version of the Penson-Kolb-Hubbard model on a linear chain. An interesting feature of the model is the absence of particle-hole symmetry around $n=1$. The model displays fractional statistical properties which manifest in the several thermodynamic responses we have examined. In particular, we draw attention to the fact that the fractional elementary excitations, which follow directly from the map of the model onto an ideal exclusion gas, are essential to clarify the nature of various physical properties of the system. For instance, the divergence of the GS charge compressibility signals the presence of strong degeneracy in the distribution of occupation of exclusons in k space; further, a striking feature of this entropic phase is the U-dependent effective electric charge associated with a nontrivial step singularity in the Fermi surface.

We have also calculated the Helmholtz free energy in the vicinity of the several U-driven quantum phase transitions exhibited by the system, thus allowing us to determine their universality classes, including several U- and n-dependent logarithmic corrections, as well as T-dependent logarithmic singularities. In particular, for the U-driven MMT associated with the dynamic exponent $z=1$, we mention the superlinear temperature dependence $T\ln^2 T$ in the quantum critical behavior of the specific heat at the critical lines $U=U_{c1}=-2t\cos(n\pi/2)$ and $U=U_{c2}=-2t\cos(n\pi)$. Moreover, the Pauli spin susceptibility is strongly enhanced by a T-dependent logarithmic singularity at $U=U_{c1}$; while at $U=U_{c2}$ the Curie term dominates the magnetic response (presence of local magnetic moments) with a negative Pauli term due to the T-dependent logarithmic singularity. Remarkably, we have also found U-dependent logarithmic correction to the specific heat near the QCP $(n=1)$ of the MIT and n-dependent logarithmic corrections to the specific heat near the MIT line $U=U_{c3}=2t$. On the other hand, both at the QCP and at the line $U=U_{c3}$, the T-dependent quantum critical behavior is in full agreement with scaling.

Finally, in the region of the GS phase diagram where *local* Cooper pair formation is most favorable, we have shown that the GS exhibits power-law superconductivity, in agreement with previous results for the Penson-Kolb model; we also stress that above half filling the pair-hopping term stabilizes local Cooper pairs in the repulsive-U regime for $U<U_{c1}$.

ACKNOWLEDGMENTS

We acknowledge the support of CNPq, FACEPE, CAPES, and FINEP (Brazilian Agencies).

APPENDIX A: DERIVATION OF EQ. (41)

In this appendix we shall prove that

$$\lim_{\substack{L\to\infty\\ N_3\to\infty}}\langle\Psi_0|c_{m\downarrow}^{\dagger}c_{m\uparrow}^{\dagger}c_{j\uparrow}c_{j\downarrow}S(m,j)|\Psi_0\rangle = 0, \quad (A1)$$

where $|\Psi_0\rangle$ is given by Eq. (37); $N_3/L=\rho$ (the density of doubly occupied sites), m and j are kept constant; and

$$S(m,j) = \frac{\left\{1 - \exp\left[\frac{i\pi}{2}\sum_{l=m}^{j-1}(n_{l\uparrow} + n_{l\downarrow})\right]\right\}}{2}. \tag{A2}$$

The introduction of the numerical factor 2 in the denominator of Eq. (A2) is a matter of convenience.

We begin by noting that

$$S(m,j)|n_1\downarrow\uparrow, n_2\downarrow\uparrow, \ldots, n_{N_3}\downarrow\uparrow\rangle = |n_1\downarrow\uparrow, n_2\downarrow\uparrow, \ldots, n_{N_3}\downarrow\uparrow\rangle, \tag{A3}$$

if there is an odd number of doubly occupied sites between m and $j-1$. Otherwise, $S(m,j)|n_1\downarrow\uparrow, n_2\downarrow\uparrow, \ldots, n_{N_3}\downarrow\uparrow\rangle = 0$. Therefore,

$$\begin{aligned} S(m,j)|\Psi_0\rangle = &\left(\frac{1}{\sqrt{L}}\right)^{N_3} \\ &\times \sum_{\{n_i\}}{}' \{\det(k_1, k_2, \ldots, k_{N_3}; n_1, n_2, \ldots, n_{N_3}) \\ &\times |n_1\downarrow\uparrow, n_2\downarrow\uparrow, \ldots, n_{N_3}\downarrow\uparrow\rangle\}, \end{aligned} \tag{A4}$$

where the prime in the sum indicates that only the set of integers satisfying the additional restriction discussed right below Eq. (A3) are taken. Moreover, it is easily verified that a dummy variable must be equal to j, otherwise $c_{j\uparrow}c_{j\downarrow}$ acting on $S(m,j)|\Psi_0\rangle$ would produce the null vector. So

$$\begin{aligned} &\langle\Psi_0|c^\dagger_{m\downarrow}c^\dagger_{m\uparrow}c_{j\uparrow}c_{j\downarrow}S(m,j)|\Psi_0\rangle \\ &= \left(\frac{1}{L}\right)^{N_3}\Bigg\{\sum_{n_1<n_2=j<\cdots<n_{N_3}}{}'[\det(k_1,k_2,\ldots,k_{N_3};n_1,n_2 \\ &= j,\ldots,n_{N_3}) \\ &\quad\times\det{}^*(k_1,k_2,\ldots,k_{N_3};n_1,n_3,\ldots,m,\ldots,n_{N_3})] \\ &\quad+\sum_{n_1<n_2<n_3=j<\cdots<n_{N_3}}{}'[\det(k_1,k_2,\ldots,k_{N_3};n_1,n_2,n_3 \\ &= j,\ldots,n_{N_3})\det{}^*(k_1,k_2,\ldots,k_{N_3};n_1,n_2,n_4,\ldots, \\ &\quad\times m,\ldots,n_{N_3})]+\cdots+\sum_{n_1<n_2<\cdots<n_j=j<\cdots<n_{N_3}}{}' \\ &\quad\times[\det(k_1,k_2,\ldots,k_{N_3};1,2,\ldots,j-1,j,\ldots,n_{N_3}) \\ &\quad\times\det{}^*(k_1,k_2,\ldots,k_{N_3};1,2,\ldots,m,\ldots,j,\ldots,n_{N_3})]\Bigg\}. \end{aligned} \tag{A5}$$

The above sums cannot be evaluated in closed form so in this point we make use of the approximation

$$\begin{aligned} &|\det(k_1,k_2,\ldots,k_{N_3};n_1,n_2,\ldots,j,\ldots,n_{N_3}) \\ &\quad\times\det{}^*(k_1,k_2,\ldots,k_{N_3};n_1,n_2,\ldots,m,\ldots,n_{N_3})| \\ &\quad\simeq|\det(k_1,k_2,\ldots,k_{N_3};n_1,n_2,\ldots,j=m,\ldots,n_{N_3})|^2, \end{aligned} \tag{A6}$$

which is justified in view of the mapping Eq. (39) and the fact that the correlation function $G_c(j,m)$, Eq. (42), decays as $1/|j-m|^2$. We thus proceed to find a majorant M so that

$$|\det(k_1,k_2,\ldots,k_{N_3};n_1,n_2,\ldots,n_{N_3})|^2 \le M \tag{A7}$$

for all set $\{n_i\}$ of N_3 integers. It follows from Eq. (37) that

$$\frac{|\det(k_1,k_2,\ldots,k_{N_3};n_1,n_2,\ldots,n_{N_3})|^2}{L^{N_3}} \tag{A8}$$

is the probability of finding paired carriers in the sites $n_1,n_2,\ldots,n_{N_3}$. So, we identify the probability Eq. (A8) to M/L^{N_3}, which implies

$$\frac{M}{L^{N_3}}\sum_{1\le n_1<n_2<\cdots<n_{N_3}\le L}(1) = 1, \tag{A9}$$

and thus

$$M = \frac{L^{N_3}}{\binom{L}{N_3}} = e^{L(1-\rho)\ln(1-\rho)}e^{N_3\ln N_3} \tag{A10}$$

for $L,N_3\to\infty$. We now return to Eq. (A5) in order to obtain

$$\begin{aligned} &|\langle\Psi_0|c^\dagger_{m\downarrow}c^\dagger_{m\uparrow}c_{j\uparrow}c_{j\downarrow}S(m,j)|\Psi_0\rangle| \\ &\quad\le e^{L(1-\rho)\ln(1-\rho)}\rho^{N_3}\Bigg\{\sum_{n_1<n_2=j<n_3<\cdots<n_{N_3}}{}'(1) \\ &\qquad+\sum_{n_1<n_2<n_3=j<\cdots<n_{N_3}}{}'(1)+\cdots \\ &\qquad+\sum_{n_1<n_2<\cdots<n_j=j<\cdots<n_{N_3}}{}'(1)\Bigg\}. \end{aligned} \tag{A11}$$

Each sum is equal to the total number of combinations of L elements N_3 such that there is an odd number of elements between m and $j-1$, and $n_p=j(p=2,3,\ldots,j)$. This total number of combinations can be written as

$$H(j,m,p)\binom{L-j}{N_3-p}, \tag{A12}$$

where $H(j,m,p)$ is a L-independent function. We now return to Eq. (A11)

$$\begin{aligned} |\langle\Psi_0|c^\dagger_{m\downarrow}c^\dagger_{m\uparrow}c_{j\uparrow}c_{j\downarrow}S(m,j)|\Psi_0\rangle| &\le e^{L(1-\rho)\ln(1-\rho)}\rho^{N_3} \\ &\times\sum_{p=2}^{j}H(j,m,p)\binom{L-j}{N_3-p}. \end{aligned} \tag{A13}$$

In the thermodynamic limit, one has

$$\binom{L-j}{N_3-p} = \frac{e^{-L(1-\rho)\ln(1-\rho)}e^{(j-p)\ln(1-\rho)}}{\rho^{N_3}}e^{-pL[1-(\ln N_3)/L]} \tag{A14}$$

so that

$$0 \le |\langle\Psi_0|c^\dagger_{m\downarrow}c^\dagger_{m\uparrow}c_{j\uparrow}c_{j\downarrow}S(m,j)|\Psi_0\rangle| \le \sum_{p=2}^{j} H(j,m,p)e^{(j-p)\ln(1-\rho)}e^{-pL[1-(\ln N_3)/L]}. \tag{A15}$$

Now it is clear that

$$\lim_{\substack{L\to\infty \\ N_3\to\infty}} \langle\Psi_0|c^\dagger_{m\downarrow}c^\dagger_{m\uparrow}c_{j\uparrow}c_{j\downarrow}S(m,j)|\Psi_0\rangle = 0. \tag{A16}$$

Notwithstanding the approximation Eq. (A6), we argue that this result remains exact in view of the exponentially small dependence $e^{-[\cdots]L}$ in Eq. (A15).

APPENDIX B: DERIVATION OF μ AND F IN REGION (II)

In this derivation, it is tacitly assumed that k_BT is less than any significant energy scale. The chemical potential is obtained as the solution of Eq. (87). As already mentioned, at $T=0$ one has $\mu_2=U$. So, finite-temperature corrections to μ_2 are obtained by using

$$\mu_2(T,n) = U + \delta\mu \tag{B1}$$

in the above equation. The substitution leads to the expression

$$(x+x^2)\int_{-2t}^{2t}\frac{\sigma(\varepsilon)d\varepsilon}{e^{\beta(\varepsilon-U)}+y} = \frac{n}{2}, \tag{B2}$$

where

$$x \equiv e^{\beta\delta\mu}, \quad y \equiv 2x + x^2, \tag{B3}$$

and $\sigma(\varepsilon)$ is defined by Eq. (86). After integrating Eq. (B2) *à la* Sommerfeld, we obtain

$$\left(\frac{x+1}{x+2}\right)\left\{n^* + k_BT\sigma(U)\ln y + \frac{\sigma'(U)}{2}(k_BT)^2\left[\frac{\pi^2}{3} + \ln^2(y)\right] + \cdots\right\} = \frac{n}{2}. \tag{B4}$$

We now expand $\delta\mu$ in a Taylor series in k_BT

$$\delta\mu = (k_BT)B_1 + (k_BT)^2B_2 + \cdots, \tag{B5}$$

and after placing Eq. (B5) in Eq. (B4) we arrive at

$$B_1 = \ln\left(\frac{2(n-n^*)}{2n^*-n}\right) \tag{B6}$$

and

$$B_2 = -\frac{n\sigma(U)}{(n-n^*)(2n^*-n)}\ln\left(\frac{4(n-n^*)n^*}{(2n^*-n)^2}\right). \tag{B7}$$

Now, F_2 can be calculated up to $\mathcal{O}(k_BT)^2$ by eliminating μ_2 in favor of n via Eq. (87)

$$\frac{F_2}{L} = n\mu_2 + \frac{\Omega}{L} = n(U+\delta\mu) - \frac{1}{\beta}\int_{-2t}^{2t}d\varepsilon\sigma(\varepsilon)\ln[1+ye^{-\beta(\varepsilon-U)}] = (n-n^*)U - \frac{1}{\pi}\sqrt{4t^2-U^2} + k_BT\left\{n\ln\left[\frac{2(n-n^*)}{2n^*-n}\right] - n^*\ln\left[\frac{4(n-n^*)n^*}{(2n^*-n)^2}\right]\right\} - \frac{(k_BT)^2}{2\pi\sqrt{4t^2-U^2}} \times\left\{\frac{\pi^2}{3} + \ln^2\left[\frac{4(n-n^*)n^*}{(2n^*-n)^2}\right]\right\} + \cdots, \tag{B8}$$

after integrating twice by parts *à la* Sommerfeld.

APPENDIX C: DERIVATION OF EQ. (99)

The first step is to calculate the chemical potential at $U=U_{c1}$. We begin by noting that at $T=0$ one has $\mu_{U_{c1}}=-2t\cos(n\pi/2)=U_{c1}$, which is obtained from Eq. (30) by taking the limit $U\to U_{c1}^-$. Next we use

$$\mu_{U_{c1}}(T,n) = U_{c1} + \delta\mu \tag{C1}$$

at finite temperatures and proceed as described in Appendix B to obtain an equation identical to Eq. (B4) with $n^*=n/2$ and $U=U_{c1}$. However, it should be stressed that since k_BT now dominates the energy scale, we have a singular behavior for x

$$\lim_{T\to 0}(1/x) = 0. \tag{C2}$$

In fact, it turns out that $x=\mathcal{O}(k_BT)^{-1}$. Therefore, by neglecting terms of $\mathcal{O}(k_BT)^2$ in Eq. (B4) (with the changes discussed above), we proceed to solve the simplified equation $x\ln x = n/[4k_BT\sigma(U_{c1}))] = \pi tn\sin(n\pi/2)/(2k_BT) \equiv A$, whose solution r is calculated by iteration: $r=A/(\lim_{l\to\infty}\alpha_l)$, where α_l is defined right below Eq. (100). We now go on by writing the solution of Eq. (B4) in the form $x=r+\delta r$. It is straightforward to get

$$\delta r = -\frac{4k_B\ \mathrm{Tr}\ \sigma(U_{c1})(1-\ln r) + 2n + \sigma'(U_{c1})(k_BT)^2r^2\left[\frac{\pi^2}{3} + \ln^2(r^2)\right]}{4k_B\ \mathrm{Tr}\ \sigma(U_{c1}) + n}. \tag{C3}$$

We are now in a position to obtain $\delta\mu$ up to $\mathcal{O}(k_BT)^2$

$$e^{\beta\delta\mu} = r\left(1 + \frac{\delta r}{r} + \cdots\right) \tag{C4}$$

so that

$$\delta\mu = k_BT \ln r + \frac{k_BT}{r}\delta r + \cdots. \tag{C5}$$

Next we calculate $F_{U_{c1}}$

$$\frac{F_{U_{c1}}}{L} = n\left(U_{c1} + k_BT \ln r + \frac{k_BT}{r}\delta r\right) - \frac{1}{\beta}\int_{-2t}^{2t} d\varepsilon\sigma(\varepsilon)\ln[1 + pe^{-\beta(\varepsilon - U_{c1})}] + \cdots, \tag{C6}$$

where $p=2re^{\delta r/r}+r^2e^{2\delta r/r}$. After integrating twice by parts *à la* Sommerfeld, we obtain

$$\frac{F_{U_{c1}}}{L} = -nt\cos(n\pi/2) - \frac{2t}{\pi}\sin(n\pi/2) - \frac{nk_BT}{r} - \frac{(k_BT)^2}{4\pi t\sin(n\pi/2)}\left[\frac{\pi^2}{3} + \ln^2(r^2)\right] + \cdots, \tag{C7}$$

which does not depend on δr.

APPENDIX D: DERIVATION OF EQ. (116)

The calculation of the chemical potential at $U=U_{c2}$ is quite similar to that presented in Appendix C. By using

$$\mu_{U_{c2}} = -2t\cos(n\pi) + \delta\mu \tag{D1}$$

in Eq. (B2), where $\delta\mu$ stands for finite-temperature corrections to $\mu_{U_{c2}}$, we find after integrating *à la* Sommerfeld an equation identical to Eq. (B4) with $n^*=n$ and $U=U_{c2}$. As in Appendix C, k_BT dominates the energy scale and thus we also obtain a singular behavior for x

$$\lim_{T\to 0} x = 0. \tag{D2}$$

Using $x=x_1+x_2$, where $x_1=\mathcal{O}(k_BT)$ and $x_2=\mathcal{O}(k_BT)^2$, one obtains

$$\frac{x+1}{x+2} = \frac{1}{2} + \frac{x_1}{4} + \frac{2x_2 - x_1^2}{8} + \mathcal{O}(k_BT)^3 \tag{D3}$$

and

$$\ln y = \ln(2x_1) + \frac{x_1}{2} + \frac{x_2}{x_1} + \mathcal{O}(k_BT)^2. \tag{D4}$$

By inserting these expansions into Eq. (B4) (with the changes discussed above), we find

$$x_1 = -\frac{k_BT\ln(2x_1)}{n\pi t\sin(n\pi)}, \tag{D5}$$

whose solution is written right below Eq. (116) and

$$x_2 = \frac{nx_1^2 - 2(k_BT)x_1[1 + \ln(2x_1)]\sigma(U_{c2}) - 2\sigma'(U_{c2})(k_BT)^2\left[\frac{\pi^2}{3} + \ln^2(2x_1)\right]}{\frac{4k_BT\sigma(U_{c2})}{x_1} + 2n}. \tag{D6}$$

Therefore, $F_{U_{c2}}$ is given by

$$\frac{F_{U_{c2}}}{L} = n[U_{c2} + k_BT\ln(x_1+x_2)] - \frac{1}{\beta}\int_{-2t}^{2t} d\varepsilon\sigma(\varepsilon)\ln[1 + ye^{-\beta(\varepsilon - U_{c2})}] + \cdots. \tag{D7}$$

After integrating twice by parts *à la* Sommerfeld, we get

$$\frac{F_{U_{c2}}}{L} = -\frac{2t}{\pi}\sin(n\pi) - nk_BT\ln 2 - \frac{nk_BTx_1}{2} - \frac{(k_BT)^2}{4\pi t\sin(n\pi)}\left[\frac{\pi^2}{3} + \ln^2(2x_1)\right] + \cdots. \tag{D8}$$

APPENDIX E: DERIVATION OF $F\sim T^{3/2}$ AT $U=U_{c3}$

First we calculate the chemical potential

$$\mu_{U_{c3}} = 2t + \delta\mu, \tag{E1}$$

where $\delta\mu$ denotes finite-temperature corrections. Equation (B2) for $U=2t$ is the starting point to calculate $\delta\mu$. After integrating it by parts, one obtains

$$\int_{-2t}^{2t} \frac{\beta e^{\beta(\varepsilon-2t)}[(1/\pi)\arccos(-\varepsilon/2t)]d\varepsilon}{[e^{\beta(\varepsilon-2t)} + y]^2} = \frac{(n-2)x + n}{2x(x+1)^2}. \tag{E2}$$

So, unless ε is very close to $2t$, the integrand is utterly negligible at low temperatures. This property allows us to make use of the expansion

$$\frac{1}{\pi}\arccos(-\varepsilon/2t) = 1 - \frac{1}{\pi}\left(\frac{2t-\varepsilon}{t}\right)^{1/2} + \cdots, \quad \varepsilon \to 2t^{-}. \tag{E3}$$

Inserting this into Eq. (E2) and making the change in variable $\theta=\beta(2t-\varepsilon)$, we obtain after neglecting exponentially small terms

$$\frac{(2-n)x^2 + (4-3n)x + 2(1-n)}{2x(x+2)(x+1)^2} = \frac{1}{\pi}\left(\frac{k_BT}{t}\right)^{1/2}\int_0^\infty \frac{e^{-\theta}\sqrt{\theta}d\theta}{(e^{-\theta}+y)^2} + \mathcal{O}(k_BT/t)^{3/2}. \tag{E4}$$

First, we consider the case $n>1$ so that Eq. (E4) can be solved by iteration

$$x = x_0 + A\left(\frac{k_BT}{t}\right)^{1/2} + \cdots, \tag{E5}$$

where

$$x_0 = \frac{2(n-1)}{2-n} \tag{E6}$$

and

$$A = \frac{8n(n-1)}{\pi(2-n)^4}\int_0^\infty \frac{e^{-\theta}\sqrt{\theta}d\theta}{(e^{-\theta}+2x_0+x_0^2)^2}. \tag{E7}$$

In this case, $F_{U_{c3}}$ reads

$$\frac{F_{U_{c3}}}{L} = n\left[2t + k_BT\ln\left(x_0 + A\sqrt{\frac{k_BT}{t}}\right)\right] - 2t - k_BT\ln y - \frac{1}{\beta}\int_{-2t}^{2t} d\varepsilon\sigma(\varepsilon)\ln[1+(1/y)e^{\beta(\varepsilon-2t)}] + \cdots. \tag{E8}$$

Since the integrand is exponentially small away from $\varepsilon=2t$, we can use the expansion

$$\sigma(\varepsilon) = \frac{1}{2\pi\sqrt{t}\sqrt{2t-\varepsilon}} + \cdots \tag{E9}$$

in the integral to capture the dominant term

$$\frac{F_{U_{c3}}}{L} = 2t(1-n) + [n\ln x_0 - \ln y_0]k_BT - \frac{t}{2\pi}\left(\frac{k_BT}{t}\right)^{3/2}\int_0^{+\infty}\frac{d\theta}{\sqrt{\theta}}\ln(1+e^{-\theta}/y_0) + \cdots, \tag{E10}$$

where $y_0=2x_0+x_0^2=4(n-1)/(2-n)^2$.

Let us now return to Eq. (E4). For $n=1$, one has

$$\frac{1}{2(x+2)(x+1)} = \frac{1}{\pi}\left(\frac{k_BT}{t}\right)^{1/2}\int_0^\infty \frac{e^{-\theta}\sqrt{\theta}d\theta}{(e^{-\theta}+y)^2} + \mathcal{O}(k_BT/t)^{3/2}. \tag{E11}$$

It should be noticed that $x,y\to 0$ as $T\to 0$. In this case

$$\int_0^\infty \frac{e^{-\theta}\sqrt{\theta}d\theta}{(e^{-\theta}+y)^2} \sim -\frac{\ln y}{y}, \tag{E12}$$

and therefore

$$x \sim \left(\frac{k_BT}{t}\right)^{1/2}\ln\left(\frac{k_BT}{t}\right). \tag{E13}$$

We now calculate $F_{U_{c3}}$ at $n=1$

$$\frac{F_{U_{c3}}}{L} = 2t + k_BT\ln x - \frac{1}{\beta}\int_{-2t}^{2t} d\varepsilon\sigma(\varepsilon)\ln[1+ye^{-\beta(\varepsilon-2t)}] = -k_BT\ln(2+x) - k_BT\int_{-2t}^{2t} d\varepsilon\sigma(\varepsilon)\ln[1+(1/y)e^{\beta(\varepsilon-2t)}] + \cdots. \tag{E14}$$

Finally, after inserting the expansion Eq. (E9) and the asymptotic form in Eq. (E13) into Eq. (E14), we obtain $F_{sing,U_{c3}}/L \sim T^{3/2}$.

[1] F. D. M. Haldane, Phys. Rev. Lett. **67**, 937 (1991).
[2] Y. S. Wu, Phys. Rev. Lett. **73**, 922 (1994); **74**, 3906 (1995).
[3] A. K. Rajagopal, Phys. Rev. Lett. **74**, 1048 (1995); **75**, 2452 (1995).
[4] S. B. Isakov, Phys. Rev. Lett. **73**, 2150 (1994); **74**, 1493 (1995).
[5] M. V. N. Murthy and R. Shankar, Phys. Rev. Lett. **73**, 3331 (1994); see also A. Dasnières de Veigy and S. Ouvry, *ibid.* **75**, 352 (1995); M. V. N. Murthy and R. Shankar, *ibid.* **75**, 353 (1995).
[6] D. Bernard and Y. S. Wu, in *Proceedings of the Sixth Nankai Workshop*, edited by M. L. Ge and Y. S. Wu (World Scientific, Singapore, 1995).
[7] Z. N. C. Ha, Nucl. Phys. B **435**, 604 (1995); *Quantum Many-Body Systems in One Dimension* (World Scientific, Singapore, 1996).
[8] Y. Hatsugai, M. Kohmoto, T. Koma, and Y. S. Wu, Phys. Rev. B **54**, 5358 (1996).
[9] S. He, X. C. Xie, and F. C. Zhang, Phys. Rev. Lett. **68**, 3460 (1992); J. Yang and W. P. Su, *ibid.* **70**, 1163 (1993); J. Yang, Phys. Rev. B **49**, 16765 (1994); **50**, 11196 (1994); M. D. Johnson and G. S. Canright, *ibid.* **49**, 2947 (1994); W. P. Su, Y. S. Wu, and J. Yang, Phys. Rev. Lett. **77**, 3423 (1996); Y. S. Wu, Y. Yu, Y. Hatsugai, and M. Kohmoto, Phys. Rev. B **57**, 9907 (1998).
[10] Y. S. Wu and Y. Yu, Phys. Rev. Lett. **75**, 890 (1995); Y. S. Wu, Y. Yu, and H. X. Yang, Nucl. Phys. B **604**, 551 (2001).
[11] C. Nayak and F. Wilczek, Phys. Rev. Lett. **73**, 2740 (1994).
[12] L. G. C. Rego and G. Kirczenow, Phys. Rev. B **59**, 13080 (1999); I. V. Krive and E. R. Mucciolo, *ibid.* **60**, 1429 (1999); S. B. Isakov, T. Martin, and S. Ouvry, Phys. Rev. Lett. **83**, 580

(1999); G. Gomila and L. Reggiani, Phys. Rev. B **63**, 165404 (2001); Physica B **314**, 141 (2002).
[13] T. H. Hansson, J. M. Leinaas, and S. Viefers, Phys. Rev. Lett. **86**, 2930 (2001); S. Viefers, T. H. Hansson, and J. M. Leinaas, J. Phys. B **34**, 4609 (2001).
[14] J. L. Riccardo, A. J. Ramirez-Pastor, and F. Roma, Phys. Rev. Lett. **93**, 186101 (2004).
[15] Y. Kato and Y. Kuramoto, J. Phys. Soc. Jpn. **65**, 77 (1996); **65**, 1622 (1996).
[16] H. Ujino and M. Wadati, J. Phys. Soc. Jpn. **65**, 1203 (1996).
[17] C. Pépin and A. M. Tsvelik, Phys. Rev. Lett. **82**, 3859 (1999).
[18] C. Vitoriano, L. B. Bejan, A. M. S. Macêdo, and M. D. Coutinho-Filho, Phys. Rev. B **61**, 7941 (2000); **62**, 10569 (2000). For the attractive case see C. Vitoriano, K. Rocha, Jr., and M. D. Coutinho-Filho, *ibid.* **72**, 165109 (2005).
[19] M. T. Batchelor and X.-W. Guan, Phys. Rev. B **74**, 195121 (2006); M. T. Batchelor, X.-W. Guan, and N. Oelkers, Phys. Rev. Lett. **96**, 210402 (2006).
[20] M. T. Batchelor and X.-W. Guan, Laser Phys. Lett. **4**, 77 (2007).
[21] R. K. Bhaduri, M. V. N. Murthy, and M. K. Srivastava, J. Phys. B **40**, 1775 (2007).
[22] X. W. Guan, M. T. Batchelor, C. Lee, and M. Bortz, Phys. Rev. B **76**, 085120 (2007).
[23] H. Katsura and Y. Hatsuda, J. Phys. A: Math. Theor. **40**, 13931 (2007).
[24] F. M. D. Pellegrino, G. G. N. Angilella, N. H. March, and R. Pucci, Phys. Rev. E **76**, 061123 (2007).
[25] D. Schuricht, J. Phys. A: Math. Theor. **41**, 015208 (2008).
[26] C. Vitoriano and M. D. Coutinho-Filho, Phys. Rev. Lett. **102**, 146404 (2009), and references therein.
[27] J. Hubbard, Proc. R. Soc. London, Ser. A **276**, 238 (1963); M. C. Gutzwiller, Phys. Rev. Lett. **10**, 159 (1963).
[28] P. W. Anderson, Science **235**, 1196 (1987); *The Theory of Superconductivity in the High-T_c Cuprates* (Princeton University Press, Princeton, 1997).
[29] J. G. Bednorz and K. A. Müller, Z. Phys. B: Condens. Matter **64**, 189 (1986).
[30] A. Hui and S. Doniach, Phys. Rev. B **48**, 2063 (1993).
[31] B. Bhattacharyya and G. K. Roy, J. Phys.: Condens. Matter **7**, 5537 (1995).
[32] A. Belkasri and F. D. Buzatu, Phys. Rev. B **53**, 7171 (1996).
[33] G. I. Japaridze and E. Müller-Hartmann, J. Phys.: Condens. Matter **9**, 10509 (1997); see also G. I. Japaridze and S Sarkar, Eur. Phys. J. B **28**, 139 (2002).
[34] S. Robaszkiewicz and B. R. Bułka, Phys. Rev. B **59**, 6430 (1999).
[35] F. Dolcini and A. Montorsi, Phys. Rev. B **62**, 2315 (2000).
[36] K. A. Penson and M. Kolb, Phys. Rev. B **33**, 1663 (1986).
[37] I. Affleck and J. B. Marston, J. Phys. C **21**, 2511 (1988).
[38] A. E. Sikkema and I. Affleck, Phys. Rev. B **52**, 10207 (1995).
[39] M. van den Bossche and M. Caffarel, Phys. Rev. B **54**, 17414 (1996).
[40] G. K. Roy and B. Bhattacharyya, Phys. Rev. B **55**, 15506 (1997).
[41] W. R. Czart and S. Robaszkiewicz, Phys. Rev. B **64**, 104511 (2001); see also, S. Robaszkiewicz and W. R. Czart, Phys. Status Solidi B **236**, 416 (2003); W. R. Czart, S. Robaszkiewicz, and B. Tobijaszewska, *ibid.* **244**, 2327 (2007).
[42] K. H. Yang, G. S. Tian, and R. Q. Han, Commun. Theor. Phys. **39**, 607 (2003).
[43] C. N. Yang, Phys. Rev. Lett. **63**, 2144 (1989); see also C. N. Yang and S. C. Zhang, Mod. Phys. Lett. B **4**, 759 (1990); S. C. Zhang, Phys. Rev. Lett. **65**, 120 (1990).
[44] The inclusion of next-nearest-neighbor hopping term can lead to unconventional superconducting GS in two- and three-dimensional lattice systems, S. Raghu, S. A. Kivelson, and D. J. Scalapino, Phys. Rev. B **81**, 224505 (2010).
[45] F. H. L. Essler, V. E. Korepin, and K. Schoutens, Phys. Rev. Lett. **67**, 3848 (1991); F. H. L. Eßler, V. E. Korepin, and K. Schoutens, Nucl. Phys. B **384**, 431 (1992).
[46] R. R. P. Singh and R. T. Scalettar, Phys. Rev. Lett. **66**, 3203 (1991); J. Stein and R. Oppermann, Phys. Rev. B **46**, 8409 (1992); S. Q. Shen and Z. M. Qiu, Phys. Rev. Lett. **71**, 4238 (1993); J. de Boer and A. Schadschneider, *ibid.* **75**, 4298 (1995); A. Montorsi and D. K. Campbell, Phys. Rev. B **53**, 5153 (1996).
[47] F. H. L. Essler, V. E. Korepin, and K. Schoutens, Phys. Rev. Lett. **68**, 2960 (1992); **70**, 73 (1993); J. de Boer, V. E. Korepin, and A. Schadschneider, *ibid.* **74**, 789 (1995).
[48] C. Wu, J. P. Hu, and S. C. Zhang, Phys. Rev. Lett. **91**, 186402 (2003); H. Zhai, Phys. Rev. B **71**, 012512 (2005).
[49] H. Fan and S. Lloyd, J. Phys. A **38**, 5285 (2005).
[50] A. Ptok, M. M. Maśka, and M. Mierzejewski, J. Phys.: Condens. Matter **21**, 295601 (2009).
[51] F. Dolcini and A. Montorsi, Phys. Rev. B **63**, 121103(R) (2001); **65**, 155105 (2002).
[52] See Ref. 41 and references therein.
[53] F. Woynarovich and K. Penc, Z. Phys. B: Condens. Matter **85**, 269 (1991).
[54] F. D. M. Haldane, J. Phys. C **14**, 2585 (1981), Table 1.
[55] W. J. Caspers and P. L. Iske, Physica A **157**, 1033 (1989); A. Schadschneider, Phys. Rev. B **51**, 10386 (1995).
[56] N. Byers and C. N. Yang, Phys. Rev. Lett. **7**, 46 (1961).
[57] B. S. Shastry and B. Sutherland, Phys. Rev. Lett. **65**, 243 (1990).
[58] A. Gendiar, R. Krcmar, and M. Weyrauch, Phys. Rev. B **79**, 205118 (2009).
[59] M. A. Continentino, *Quantum Scaling in Many-Body Systems* (World Scientific, Singapore, 2001). See also M. A. Continentino and M. D. Coutinho-Filho, Solid State Commun. **90**, 619 (1994).
[60] H. Bluhm, N. C. Koshnick, J. A. Bert, M. E. Huber, and K. A. Moler, Phys. Rev. Lett. **102**, 136802 (2009); A. C. Bleszynski-Jayich, W. E. Shanks, B. Peaudecerf, E. Ginossar, F. von Oppen, L. Glazman, and J. G. E. Harris, Science **326**, 272 (2009).
[61] M. Büttiker, Y. Imry, and R. Landauer, Phys. Lett. A **96**, 365 (1983); see also H. Bary-Soroker, O. Entin-Wohlman, and Y. Imry, Phys. Rev. Lett. **101**, 057001 (2008), and references therein.
[62] See, e.g., K. Huang, *Statistical Mechanics* (Wiley, Singapore, 1987), Chap. 7.
[63] F. D. M. Haldane, in *Perspectives in Many-Particle Physics*, Proceedings of the International School of Physics "Enrico Fermi," Course 121, Varenna, 1992, edited by J. R. Schrieffer and R. A. Broglia (North-Holland, New York, 1994), Chap. 1.
[64] H. Shiba and P. A. Pincus, Phys. Rev. B **5**, 1966 (1972).
[65] A. Anfossi, P. Giorda, A. Montorsi, and F. Traversa, Phys. Rev. Lett. **95**, 056402 (2005); A. Anfossi, P. Giorda, and A. Montorsi, Phys. Rev. B **75**, 165106 (2007).